doi:10.1093/brain/awt294 Brain 2014: 137; 153–171 | 153

BRAIN
A JOURNAL OF NEUROLOGY

Abnormal autonomic and associated brain activities during rest in autism spectrum disorder

Tehila Eilam-Stock,[1,2,3] Pengfei Xu,[4] Miao Cao,[4] Xiaosi Gu,[5,6] Nicholas T. Van Dam,[1,3] Evdokia Anagnostou,[3,7] Alexander Kolevzon,[3,7] Latha Soorya,[3,7] Yunsoo Park,[3] Michael Siller,[8] Yong He,[4] Patrick R. Hof[9] and Jin Fan[1,2,3,7,9]

1 Department of Psychology, Queens College, City University of New York, Flushing, NY 11367, USA
2 The Graduate Centre, City University of New York, New York, NY 10016, USA
3 Department of Psychiatry, Icahn School of Medicine at Mount Sinai, New York, NY 10029, USA
4 State Key Laboratory of Cognitive Neuroscience and Learning and International Data Group/McGovern Institute for Brain Research, Beijing Normal University, Beijing, 100875, China
5 Wellcome Trust Centre for Neuroimaging, University College London, London WC1N 3BG, UK
6 Virginia Tech Carilion Research Institute, Roanoke, VA 24016, USA
7 Seaver Autism Centre for Research and Treatment, Icahn School of Medicine at Mount Sinai, New York, NY 10029, USA
8 Department of Psychology, Hunter College, City University of New York, New York, NY 10065, USA
9 Fishberg Department of Neuroscience and Friedman Brain Institute, Icahn School of Medicine at Mount Sinai, New York, NY 10029, USA

Correspondence to: Jin Fan, PhD,
Department of Psychology,
Queens College,
City University of New York,
Flushing,
NY 11367,
USA
E-mail: jin.fan@qc.cuny.edu

Autism spectrum disorders are associated with social and emotional deficits, the aetiology of which are not well understood. A growing consensus is that the autonomic nervous system serves a key role in emotional processes, by providing physiological signals essential to subjective states. We hypothesized that altered autonomic processing is related to the socio-emotional deficits in autism spectrum disorders. Here, we investigated the relationship between non-specific skin conductance response, an objective index of sympathetic neural activity, and brain fluctuations during rest in high-functioning adults with autism spectrum disorder relative to neurotypical controls. Compared with control participants, individuals with autism spectrum disorder showed less skin conductance responses overall. They also showed weaker correlations between skin conductance responses and frontal brain regions, including the anterior cingulate and anterior insular cortices. Additionally, skin conductance responses were found to have less contribution to default mode network connectivity in individuals with autism spectrum disorders relative to controls. These results suggest that autonomic processing is altered in autism spectrum disorders, which may be related to the abnormal socio-emotional behaviours that characterize this condition.

Keywords: autism; autonomic nervous system; emotion; skin conductance; resting state

Abbreviations: ADI-R = Autism Diagnostic Interview-Revised; ASD = autism spectrum disorders; DMN = default mode network; SCR = skin conductance response

Received March 21, 2013. Revised August 21, 2013. Accepted September 5, 2013

Introduction

Autism spectrum disorder (ASD) manifests early in development, and is characterized by deficits in social interaction and communication, as well as stereotyped and repetitive behaviours, and restricted interests in domains of activities (American Psychiatric Association, 2013). Individuals with ASD also exhibit difficulties in emotional processing, particularly in self-awareness of feelings (Hill *et al.*, 2004; Silani *et al.*, 2008) and in the interpretation of feelings of others (Hobson *et al.*, 1988; Baron-Cohen, 1991; Bal *et al.*, 2010). Despite the extensive investigation into the aetiology of ASD, the psychophysiological correlates of the socio-emotional deficits that characterize the disorder are not yet clear. Further exploration of the physiological and neural substrates of social and emotional processes is critical for better understanding, diagnosis, and treatment of ASD.

The autonomic nervous system regulates the physiological events associated with emotional experiences, including changes in heart rate, respiration, pupil dilation and sweating (Craig, 2002; Barrett *et al.*, 2007). James (1884) and Lange (1885) proposed that these physiological changes are essential precursors for the subjective feeling of emotions. This idea has since been supported and extended by studies demonstrating that different emotional stimuli generate distinct autonomic activities, which are interpreted by the brain as different emotional experiences (Ekman, 1983; Rainville *et al.*, 2006; Harrison *et al.*, 2010). False physiological feedback affects emotional attributions (Valins, 1966; Liebhart, 1977), and emotional interpretation of ambiguous stimuli (Truax, 1983; Gray *et al.*, 2007). As social situations are often ambiguous and require rapid interpretation of emotional cues, autonomic nervous system signals play a critical role in socio-emotional processing.

The initial processing of autonomic signals takes place in the reticular formation, brainstem and thalamic nuclei, and the hypothalamus, whereas higher-order processing of these signals takes place mainly in the somatosensory cortex, supplementary motor area, anterior insular cortex, and anterior cingulate cortex (Boucsein, 1992; Damasio *et al.*, 2000; Craig, 2002; Porges, 2003; Critchley, 2005). Specifically, the anterior insular cortex, through bidirectional neural connections with the thalamus, amygdala, nucleus accumbens, anterior cingulate cortex and orbitofrontal cortex, is suggested to have a critical role in the integration of bottom-up interoceptive and exteroceptive signals with top-down predictions and evaluations of emotional states (Craig, 2002, 2003; Gray *et al.*, 2007; Harrison *et al.*, 2010; Critchley *et al.*, 2011; Seth *et al.*, 2011; Gu *et al.*, 2013). The anterior insular cortex and anterior cingulate cortex are involved in socio-emotional processing (Damasio *et al.*, 2000; Adolphs, 2002; Phillips *et al.*, 2003; Frith and Frith, 2007; Gu *et al.*, 2012, 2013) in addition to their role in autonomic nervous system regulation, further supporting the important relationship between socio-emotional processing and autonomic activity. Abnormal autonomic nervous system activity may, therefore, be a potential source of the socio-emotional deficits that characterize ASD.

Physiological studies have demonstrated abnormal autonomic nervous system activity in ASD. Abnormal autonomic activity related to external stimuli has been found in individuals with ASD, particularly when those stimuli were of a social or emotional nature (Hirstein *et al.*, 2001; Kylliainen and Hietanen, 2006; Vaughan Van Hecke *et al.*, 2009). Abnormalities in basal autonomic activity have been observed in ASD as well, including reduced baseline cardiac parasympathetic activity (Ming *et al.*, 2005), lower amplitude of respiratory sinus arrhythmia (Bal *et al.*, 2010), and larger baseline pupil dilation (Anderson and Colombo, 2009; Anderson *et al.*, 2013) when compared with matched neurotypical control subjects. Gastrointestinal symptoms have also been found to be significantly more prevalent in ASD than in neurotypical samples (Horvath *et al.*, 1999; Molloy and Manning-Courtney, 2003; White, 2003). These findings of increased sympathetic and decreased parasympathetic activity suggest an imbalance between these two systems in ASD.

Autonomic activity has also been linked to functional connectivity patterns in the resting brain (Birn *et al.*, 2008; Iacovella and Hasson, 2011; Fan *et al.*, 2012; Chang *et al.*, 2013). In a recent study we showed significant contributions of skin conductance response (SCR) signal, an objective and sensitive marker of sympathetic neural activity (Vetrugno *et al.*, 2003), to the connectivity strength of the default mode network (DMN) in a healthy cohort (Fan *et al.*, 2012). Previous investigations of resting-state functional connectivity in ASD have demonstrated weaker connectivity of the DMN compared with neurotypical control subjects (Kennedy and Courchesne, 2008*b*; Monk *et al.*, 2009; Assaf *et al.*, 2010; Weng *et al.*, 2010). It is possible that these findings of weaker DMN connectivity in ASD may be explained, at least in part, by differences in autonomic nervous system activity between the groups.

We hypothesized that ASD is associated with abnormal autonomic and correlated brain activities. This may stem from alterations in the central generation of autonomic response, the peripheral conductance of autonomic nervous system signals, and/or the central representations of physiological changes. To test our hypothesis, we recorded skin conductance and simultaneously measured brain activity during rest using functional MRI from high-functioning adults with ASD, as well as from demographically matched neurotypical control subjects. We predicted that the rate of non-specific (not task-evoked) SCR would differ between the groups, and that there would be differences in brain activity and connectivity associated with SCR, such that (i) SCR would be associated with subcortical and cortical brain regions that process and modulate autonomic activity to a lesser extent in ASD compared with neurotypical controls; and (ii) differences in DMN connectivity strength between ASD and neurotypical controls could be explained, at least partially, by differences in autonomic nervous system activity.

Materials and methods

Participants

Seventeen high-functioning adults with autism ($n = 12$) or Asperger's syndrome ($n = 5$) (ASD group) and 15 matched neurotypical control participants were evaluated at the Seaver Autism Centre for Research

Table 1 Demographic data (means ± SD) of ASD and neurotypical control groups

Subject characteristics	ASD ($n = 17$)	NC ($n = 15$)	t	P
Age (years)	26.1 ± 6.5	27.1 ± 8.2	0.37	0.72
Handedness score	60.0 ± 53.40	87.3 ± 11.6	2.06	0.06
Years of education[a]	14.90 ± 2.3	16.2 ± 1.8	1.7	0.10
Parents' socio-economic status	88.35 ± 18.73	90.73 ± 23.19	0.32	0.75
Full-scale IQ	110.3 ± 18.6	112.6 ± 12.5	0.42	0.68
ASD diagnosis (autism/Asperger's)	12/5			
ADI-R[b]				
Social	18.3 ± 8.0			
Verbal communication	16.0 ± 4.8			
Repetitive behaviour	5.9 ± 3.0			
Development	3.0 ± 1.6			
ADOS-G				
Communication	3.1 ± 1.5			
Social	7.3 ± 2.6			
Imagination	0.7 ± 0.5			
Stereotyped behaviours	1.4 ± 1.4			

[a]Years of education data was not available for five participants, therefore ASD: $n = 14$, neurotypical controls (NC): $n = 13$.
[b]ADI-R scores were not available for one participant, therefore $n = 16$ for this measure.

and Treatment, Icahn School of Medicine at Mount Sinai (Table 1 for demographic data). All participants underwent a diagnostic evaluation consisting of psychiatric, medical, and developmental assessments, as well as IQ measurement using the Wechsler Adult Intelligence Scale (WAIS-III) (Wechsler, 1997). Diagnoses of autism or Asperger's syndrome were determined by psychiatric interview according to the Diagnostic and Statistical Manual for Mental Disorders, Fourth Edition (DSM-IV-TR), and confirmed by the Autism Diagnostic Observation Schedule-Generic (ADOS-G) (Lord *et al.*, 2000), as well as the Autism Diagnostic Interview-Revised (ADI-R) (Lord *et al.*, 1994). Exclusion criteria included epilepsy, history of schizophrenia, schizoaffective disorder or other Axis I mental disorders, except for obsessive-compulsive disorder (given the phenotypic overlap with ASD), and use of depot neuroleptic medication or other psychoactive drugs within the 5 weeks prior to participation. Participants who had a lifetime history of substance/alcohol dependence and/or abuse within the last year were also excluded. For the healthy control group, participants were excluded based on medical illness or history in first-degree relatives of developmental disorders, learning disabilities, autism, affective disorders, and anxiety disorders. All participants provided written informed consent, approved by the Icahn School of Medicine at Mount Sinai Institutional Review Board.

Data acquisition

Skin conductance response acquisition

SCR was acquired according to the procedure described by Fan *et al.* (2012). Briefly, SCR was recorded using the GSR100C amplifier (BIOPAC Systems), together with the base module MP150 and the AcqKnowledge software (version 3.9.1.6). The GSR100C measures skin conductance by applying a constant voltage of 0.5 V between two electrodes that are attached to the skin. This allows for the measurements of both skin conductance level and SCR, which vary with sweat gland activity due to stress, arousal or emotional excitement. Skin conductance (measured in μS) was recorded using a 2000-Hz sampling rate (gain = 2 μS/V, both high-pass filters = DC, low-pass filter = 10 Hz). After cleaning the skin with alcohol swabs, two EL507 disposable EDA (isotonic gel) electrodes were placed on the palmar surface of the distal phalanges of the big and second toes of left foot. The electrode leads were shielded and the signal was low-pass filtered (using the MRI-Compatible MRI CBL/FILTER System MECMRI-TRANS) to reduce radiofrequency interference from the scanner. BIOPAC recording was synchronized to the E-Prime (Psychology Software Tools) program through the parallel port of the computers to enable precise time alignment of skin conductance recording with scan onsets.

Image acquisition

All brain images were obtained using a 3 T Siemens Allegra MRI system at the Icahn School of Medicine at Mount Sinai, and were acquired parallel to the anterior-posterior commissures axis (AC-PC). Foam padding was used to reduce head motion. Whole-brain anatomical T_2-weighted images were acquired in high-resolution using a turbo spin-echo plus sequence: 40 axial slices of 4 mm thickness; skip = 0 mm; repetition time = 4050 ms; echo time = 99 ms; flip angle = 170°; field of view = 240 mm; matrix size = 448 × 512; voxel size = 0.47 × 0.47 × 4 mm. After the anatomical image acquisition, one run of T_2*-weighted images was obtained during rest, corresponding to the T_2-weighted images localization, using a 6 min gradient echoplanar imaging sequence for resting-state functional MRI: 40 axial slices, 4-mm thick; skip = 0 mm; repetition time = 2500 ms; echo time = 27 ms; flip angle = 82°; field of view = 240 mm; matrix size = 64 × 64; in-plane resolution = 3.75 × 3.75 mm. The resting-state functional MRI run started with two dummy volumes before the onset of the fixation to allow for equilibration of T_1 saturation effects, followed by 144 image volumes. Refer to the Supplementary material for a detailed procedure of the eyes-open resting-state scan.

Data analysis

Skin conductance analysis

Skin conductance level was calculated as the average of all data points on the skin conductance waveform for each of the participants. A

t-test was conducted between the skin conductance level values of the groups to examine possible differences in basal skin conductance levels. AcqKnowledge software (version 4.2) was used in order to identify and count SCRs (Supplementary material). The number of valid SCR events was determined for each participant, and a *t*-test was then conducted to examine possible group differences in the number of SCRs.

Regression analysis

To correlate SCR with brain fluctuations, the skin conductance waveform was down-sampled by averaging the data points in each 2.5-s bin matching the repetition time (2.5 s) of the echoplanar imaging scan of functional image acquisition. Because relaxation causes skin conductance level to decrease slowly in a linear fashion, the SCR waveform was detrended and band-pass filtered with the same frequency range (0.01–0.08 Hz) that is used in a typical resting-state functional MRI analysis. The similarity between the SCR and haemodynamic response function curves (Bach *et al.*, 2010*a*, *b*) allows for using SCR as a regressor in the model directly without transformations, using the same filtering band for both SCR and blood oxygenation level-dependent signals (0.01–0.08 Hz) (Fan *et al.*, 2012). SCR was then entered as a regressor in a general linear model (Friston *et al.*, 1995) using statistical parametric mapping package (SPM8; Wellcome Trust Centre for Neuroimaging, London, UK). Numbers of SCR were not equated between the groups to avoid specification error (Supplementary material). The echoplanar imaging scans were realigned to the first volume, timing corrected, coregistered to the T_2 image, normalized to a standard template (MNI, Montreal Neurological Institute), resampled to a $2 \times 2 \times 2$ mm voxel size, and spatially smoothed with an 8 mm full-width at half-maximum Gaussian kernel. The general linear model was then conducted with the SCR time series as a predictor of the observed blood oxygen level-dependent signals. Low-frequency drifts in signal were removed using a standard high-pass filter with a 128 s cut-off. Serial correlation was estimated using an autoregressive AR(1) model. To remove non-neural noise from the data, ventricle and white-matter signals were extracted using corresponding masks and were entered as covariates. In addition, the six parameters generated during motion correction were also entered as covariates. Head motions (for all participants) did not exceed 2.5 mm of displacement or 2.5° of rotation in any direction. Finally, mean voxel value was used for global calculation and grand mean scaling, applied with global normalization to further remove non-specific noise (Van Dijk *et al.*, 2010). Detailed justifications for using the global mean correction can be found in the Supplementary material.

The contrast images from the participants in each group were entered into a second-level random effect group analysis. The resultant voxel-wise statistical maps were thresholded for significance using a cluster-size algorithm that protects against an inflation of the false-positive rate of multiple comparisons; an uncorrected *P*-value of 0.05 for the height (intensity) threshold of each activated voxel and extent threshold of $k = 120$ was used based on Monte Carlo simulation (Slotnick and Schacter, 2004). Assuming an individual voxel type I error of $P < 0.05$, a cluster extent of 120 contiguous resampled voxels ($2 \times 2 \times 2$ mm) was indicated as necessary to correct for multiple voxel comparisons at $P < 0.05$. Statistical results were mapped onto the standardized surface of the cerebral cortex.

Functional connectivity analysis of the default mode network

To investigate the relationship between non-specific SCR and brain connectivity during rest, a functional connectivity analysis was conducted using a seed region within the posterior cingulate cortex as in previous studies (Koshino *et al.*, 2005). Specifically, time-series volumes of functional MRI scan images were preprocessed for each participant using the Data Processing Assistant for Resting-State fMRI (DPARSF) toolbox (Yan and Zang, 2010). This included slice timing correction, realignment, coregistration, normalization and spatial smoothing (using an 8 mm full-width at half-maximum Gaussian kernel) as in the regression analysis. In addition, de-trending (to remove the systematic drift) and temporal filtering (band-pass, 0.01–0.08 Hz, to reduce the effect of low-frequency drift and high-frequency physiological signal or noise) were applied. Time course of the posterior cingulate cortex (left and right combined) was then extracted using the automated anatomical labelling template (Tzourio-Mazoyer *et al.*, 2002), and a voxel-wise linear correlation between the mean time course of the posterior cingulate cortex and the time course of each voxel in the whole brain was calculated using the resting-state functional MRI data analysis toolkit (Song *et al.*, 2011). The six head motion parameters, global mean signal, white matter signal, and CSF signal were included as covariates. A two-sample *t*-test was then conducted to examine between-group connectivity differences.

To test the effects of SCR on brain connectivity, changes in functional connectivity of the posterior cingulate cortex before and after regressing out SCR effects were examined and compared between the groups in an ANOVA model. SCR signals were regressed out as covariates in a second voxel-wise connectivity analysis, followed by transformations of the correlation coefficients using Fisher's r-to-z' transformations. Posterior cingulate cortex time course was also extracted after regressing out the SCR signal. In addition, to examine SCR contributions to the posterior cingulate cortex functional connectivity within each group, a paired *t*-test was conducted for each group before versus after regressing out SCR signals for the posterior cingulate cortex functional connectivity maps. Posterior cingulate cortex connectivity analysis is reported here because it allows comparisons with previous studies investigating DMN connectivity in ASD that used a posterior cingulate cortex seed (Monk *et al.*, 2009; Weng *et al.*, 2010), and because the posterior cingulate cortex has a more focal anatomical definition than alternative seed regions. However, the ventromedial prefrontal cortex, also commonly used as a DMN seed, is potentially more relevant to ASD abnormalities, emotional processing and autonomic pathways. We, therefore, conducted an additional functional connectivity analysis for the time course of the ventromedial prefrontal cortex, using the coordinates (−1, 47, −4) reported by Fox *et al.* (2005), and group differences were examined. To further examine possible differences in the connectivity of areas that are related to emotional and autonomic signal processing, we also tested the functional connectivity of the anterior insular cortex (Supplementary material). It is important to note that there were no significant differences in head motion between the two groups, as was indicated by the root mean squares of both overall head motion displacement and rotation and the temporal derivatives (Supplementary material).

Functional connectivity analysis of the whole brain

To examine whether SCR contributes to the whole brain connectivity, a voxel-wise whole brain functional connectivity strength analysis was performed both before and after regressing out the SCR signal. Images were preprocessed using DPARSF, similar to the posterior cingulate cortex functional connectivity analysis, with two exceptions. First, the resolution of resultant echoplanar imaging was $3 \times 3 \times 3$ mm after normalization to reduce computational load. Second, to reduce artificial local correlations between voxels introduced by smoothing, a 4 mm full-width at half-maximum Gaussian kernel was used (instead of 8 mm as in the posterior cingulate cortex connectivity analysis). For

each voxel, functional connectivity strength was measured as the summed weights of all connections linking this voxel and every other voxel. Pearson correlation coefficients for the time series of every possible pair of voxels were calculated to obtain the whole brain correlation matrix for each participant. The calculation was constrained within a customized mask (n voxels = 48 159) including all voxels with grey matter tissue probability >20% on the averaged grey matter map of all participants. The functional connectivity strength (FCS) was computed for each voxel as follows:

$$FCS(i) = \frac{1}{N}\sum_{j\neq 1} z_{ij}, r_{ij} > 0.3$$

where r_{ij} is the correlation coefficient of voxel i and voxel j, z_{ij} is the normalized r_{ij} value using Fisher's r-to-z transformation, and 0.3 is the threshold set to eliminate the potential contributions of weak connections arising from noise. To evaluate the reproducibility of our results, additional functional connectivity strength maps were calculated using both 0.2 and 0.4 correlation thresholds; these computations led to no major changes in our primary results. The connectivity map was then standardized by converting to Z scores so that maps across participants could be averaged and compared. The Z score transformation is:

$$Z(i) = \frac{FCS(i) - \mu}{\sigma}, 1 \leq i \leq N,$$

where μ and σ are mean and SD of the functional connectivity strength across all the voxels in the whole-brain map.

Notably, in graph theory, the functional connectivity strength is referred to as 'degree centrality' or 'degree' of weighted networks, and voxels with high functional connectivity strength usually play important roles in information transformation (Buckner *et al.*, 2009; Cole *et al.*, 2010; Zuo *et al.*, 2012; Liang *et al.*, 2013; Wang *et al.*, 2013). To examine the SCR contribution to whole brain connectivity, functional connectivity strength maps before and after regressing out the SCR signals were compared within each group using paired t-tests. Between-group differences of SCR signal contribution to whole brain functional connectivity (i.e. functional connectivity strength maps before versus after regressing out SCR signals) were examined in an ANOVA model. All statistical maps were corrected for multiple comparisons to a significance level of $P < 0.05$ by combining the individual voxel P-value < 0.05 with cluster size >67 voxels, based on Monte Carlo simulation (Ledberg *et al.*, 1998).

Relationship between autism symptom severity, skin conductance and imaging data

Correlations between the ADI-R subscale scores of each of the ASD participants and number of SCRs and overall skin conductance level were examined. In addition, correlations between the individual ADI-R subscale scores and SCR-brain association, posterior cingulate cortex connectivity, ventromedial prefrontal cortex connectivity, and whole brain connectivity maps were examined using regression analyses. The ADI-R four subscales include ratings of social interaction (subscale A), communication (subscale B), repetitive and restricted behaviour (subscale C), and early development (subscale D). Higher scores on each scale indicate higher symptom severity in each of the specific domains. Note that these exploratory correlation analyses were not corrected for multiple comparisons.

Modelling central generation and representation of skin conductance response

The central generation and representation (feedback) of SCR were modelled by shifting the SCR vector in relation to the haemodynamic response. Two models were created: a generation model in which brain activation preceded the SCR signal by one repetition time (2.5 s), and a representation model in which SCR preceded brain activation by one repetition time (Critchley *et al.*, 2000; Patterson *et al.*, 2002) (see Supplementary material for details of the modelling).

Results

Electrodermal activity

A t-test revealed no significant difference in skin conductance level between ASD (15.96 ± 1.83 μS) and neurotypical controls [17.27 ± 1.76 μS, $t(30) = 0.51$, $P > 0.05$, two-tailed] (Fig. 1A). However, during the scan period, the ASD group had significantly less non-specific SCRs (4.76 ± 1.34) compared with the neurotypical control group [12.2 ± 3.13, $t(30) = 2.19$, $P < 0.05$, two-tailed] (Fig. 1B).

Skin conductance response and resting state brain activity

In the neurotypical control group, there were significant positive correlations between SCR and the anterior insular cortex, dorsal anterior cingulate cortex, supplementary motor area, medial prefrontal cortex, thalamus, superior parietal lobule, calcarine cortex, cuneus, and basal ganglia, as well as negative correlations with the precentral gyrus, superior parietal lobule, posterior cingulate cortex, precuneus, and inferior parietal lobule (Table 2 and Fig. 2A). In the ASD group, SCR was positively correlated with the lingual gyrus, calcarine cortex, superior and inferior parietal lobule, precentral and postcentral gyri, middle temporal gyrus, and inferior frontal gyrus, and was negatively correlated with the anterior cingulate cortex, supplementary motor area, medial prefrontal cortex, basal ganglia, inferior parietal and temporal gyri, posterior midcingulate cortex (see Vogt, 2005 for definition), and the thalamus (Table 3 and Fig. 2B). A between-group comparison

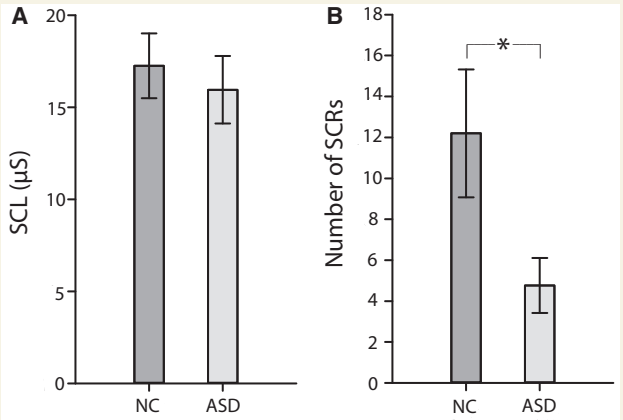

Figure 1 (**A**) Skin conductance level (SCL) and (**B**) number of skin conductance responses (SCR) during the entire rest session (6 min). NC = neurotypical controls.

Table 2 Positive and negative correlations between SCR and brain activation in neurotypical controls

Region	L/R	BA	*x*	*y*	*z*	*T*	*Z*	*P*	*k*
Positive									
Mid frontal gyrus	R	9	36	46	32	4.73	3.59	0.000	12334
Superior parietal lobule	R	7	30	−40	40	4.66	3.56	0.000	
Superior frontal gyrus	R	6	22	6	62	3.97	3.20	0.001	
Thalamus	L		−12	−4	0	3.93	3.17	0.001	
Caudate nucleus	R		12	14	18	3.87	3.14	0.001	
Thalamus	R		14	−8	12	3.82	3.11	0.001	
Caudate nucleus	L		−14	12	10	3.77	3.08	0.001	
Lateral globus pallidus	R		24	−18	−2	3.76	3.08	0.001	
Mid frontal gyrus	R	10	38	50	24	3.76	3.08	0.001	
Caudate nucleus	L		−16	18	4	3.74	3.06	0.001	
Anterior cingulate cortex	R	32	16	20	36	3.74	3.06	0.001	
Anterior cingulate cortex	L	32	−16	10	46	3.65	3.01	0.001	
Anterior cingulate cortex	R	32	6	26	38	3.61	2.99	0.001	
Anterior insular cortex	L		−34	26	8	3.59	2.97	0.001	
Anterior insular cortex	R		32	18	4	3.53	2.93	0.002	
Caudate nucleus	R		14	18	0	3.49	2.91	0.002	
Mid frontal gyrus	R	6	42	4	32	3.35	2.83	0.002	
Mid frontal gyrus	R	9	48	22	26	3.35	2.82	0.002	
Orbitofrontal cortex	R	11	26	48	−12	3.05	2.63	0.004	
Anterior insular cortex	R		32	26	6	2.97	2.57	0.005	
Mid frontal gyrus	L	10	−24	32	18	2.91	2.53	0.006	
Inferior frontal gyrus	R	44/45	58	22	4	2.88	2.51	0.006	
Putamen	R		26	18	−6	2.87	2.50	0.006	
Superior frontal gyrus	L	8	−4	24	44	2.81	2.46	0.007	
Precentral gyrus	R	6	44	0	42	2.76	2.42	0.008	
Mid temporal gyrus	R	21/22	52	−22	−2	2.70	2.39	0.009	
Supplementary motor area	R	8	2	22	50	2.32	2.10	0.018	
Inferior parietal gyrus	R	40	56	−40	52	4.38	3.42	0.000	253
Supramarginal gyrus	R	40	48	−36	42	2.66	2.36	0.009	
Dentate nucleus	L		−26	−40	−36	3.73	3.06	0.001	509
Cerebellum crus VI	L		−24	−64	−24	3.61	2.98	0.001	
Superior parietal lobule	L	7	−22	−42	42	3.67	3.02	0.001	309
Calcarine cortex	L	17	−16	−76	8	3.13	2.68	0.004	518
Cuneus	L	18	−4	−94	10	3.12	2.67	0.004	
Calcarine cortex	L	17	−12	−82	12	2.77	2.43	0.008	
Cuneus	R	18	8	−92	16	2.64	2.34	0.010	
Calcarine cortex	R	17	8	−86	10	2.61	2.32	0.010	
Lingual gyrus	L	19	−16	−74	0	2.40	2.16	0.015	
Precentral gyrus	L	6	−24	−16	62	2.34	2.12	0.017	
Negative									
Precentral gyrus	L	6	−2	−20	72	3.70	3.04	0.001	329
Precentral gyrus	R	6	6	−22	62	2.34	2.12	0.017	
Superior parietal lobule	L	7	−22	−58	58	2.76	2.42	0.008	616
Posterior cingulate gyrus	L	23	−6	−46	24	2.60	2.31	0.010	
Posterior cingulate gyrus	R	23	4	−54	22	2.60	2.31	0.011	
Precuneus	L	7	−8	−58	42	2.25	2.05	0.020	
Posterior central gyrus	R	31	12	−54	38	2.19	2.00	0.023	
Posterior cingulate gyrus	L	31	−2	−54	36	2.15	1.97	0.024	
Posterior cingulate gyrus	R	31	4	−58	30	2.02	1.86	0.031	
Inferior parietal lobule	L	40/22	−58	−42	24	2.74	2.41	0.008	133
Inferior parietal lobule	R	40	64	−22	32	2.66	2.35	0.009	161

Height threshold: T = 1.76, $P < 0.05$.
Extent threshold: k = 120.
L = left; R = right; BA = Brodmann area.

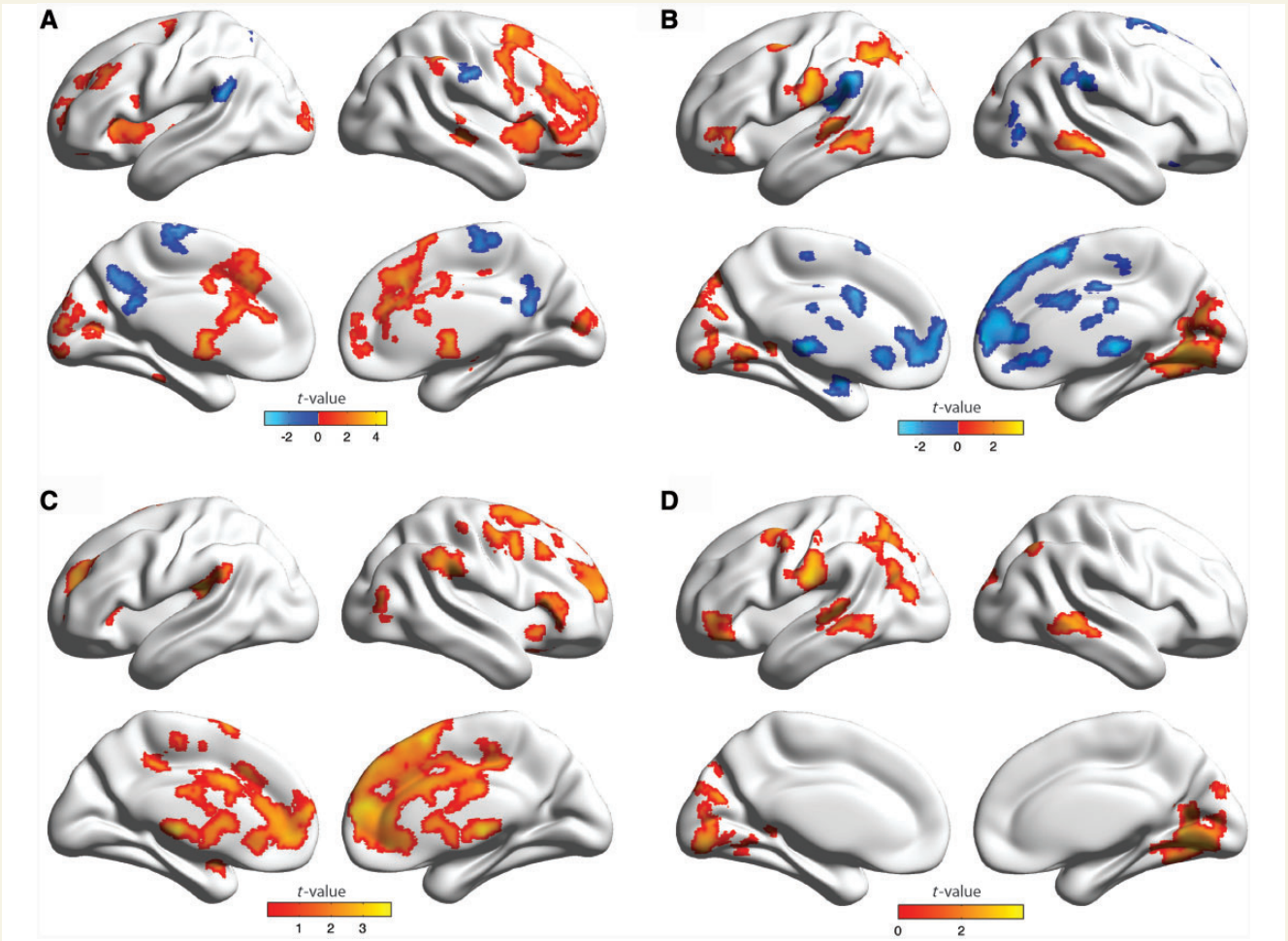

Figure 2 Positive and negative correlations between non-specific SCR and brain fluctuations during rest in (**A**) neurotypical control subjects, and (**B**) adults with ASD. Red indicates voxels with positive correlations, whereas blue indicates voxels with negative correlations. (**C**) Stronger correlations in neurotypical control subjects compared with ASD (neurotypical controls > ASD), and (**D**) stronger correlations in ASD compared with neurotypical control subjects (ASD > neurotypical controls). These hemispheric surfaces were visualized using BrainNet Viewer (http://www.nitrc.org/projects/bnv/, Xia et al., 2013).

similarly revealed that medial frontal brain regions were generally more correlated with SCR in the neurotypical control group, whereas posterior and sensory regions were generally more correlated with SCR in the ASD group (Table 4 and Fig. 2C and D).

Skin conductance response and resting state functional connectivity

Posterior cingulate cortex seed-based analysis results

Using the posterior cingulate cortex as a seed region, the neurotypical control group had stronger connectivity between the seed and areas of the DMN, compared to the ASD group, mainly with the ventromedial prefrontal cortex and the left inferior parietal lobule (Table 5 and Fig. 3A). Stronger connectivity was found in ASD between the posterior cingulate cortex and the superior and inferior occipital gyri, temporal pole, lingual gyrus, fusiform gyrus, amygdala, hippocampus, posterior insular cortex, supplementary motor area, and precentral and postcentral gyri (Table 5 and Fig. 3B). The general linear model revealed a significant interaction between group (ASD versus neurotypical control subjects) and SCR (before versus after regressing out SCR), wherein SCR had greater positive effects on the connectivity between posterior cingulate cortex and medial prefrontal and orbitofrontal cortices, precentral and postcentral gyri, supramarginal gyrus, and superior and inferior parietal gyri in neurotypical control subjects than in ASD (Table 6 and Fig. 3C). In contrast, SCR had a greater positive impact on the connectivity between the posterior cingulate cortex and the posterior insular cortex, lingual gyrus, amygdala, hippocampus, parahippocampal and fusiform gyri, superior and middle occipital gyri, and superior and inferior temporal gyri in ASD than in neurotypical control subjects (Table 6 and Fig. 3D). For paired *t*-test results within each group (before > after regressing out SCR signal), see Supplementary Table 1 and Supplementary Fig. 1. For ventromedial prefrontal cortex and anterior insular cortex functional connectivity results, see Supplementary Tables 2 and 3, and Supplementary Figs 2 and 3.

Voxel-wise whole brain connectivity

A between-group comparison revealed that the neurotypical control group had higher functional connectivity strength in the

Table 3 Positive and negative correlations between SCR and brain activation in ASD

Region	L/R	BA	x	y	z	T	Z	P	k
Positive									
Lingual gyrus	R	19	14	−58	−6	3.67	3.08	0.001	4196
Superior occipital gyrus	R	19	16	−82	20	3.48	2.96	0.002	
Lingual gyrus	R	18/19	16	−80	−4	3.44	2.93	0.002	
Calcarine cortex	L	17	−14	−82	2	3.28	2.82	0.002	
Inferior parietal lobule	L	40	−48	−50	48	3.27	2.82	0.002	
Cerebellum crus VI	R		24	−58	−26	3.21	2.78	0.003	
Superior parietal lobule	L	7	−30	−64	58	3.17	2.75	0.003	
Fusiform gyrus	L	19	−22	−62	−10	2.95	2.60	0.005	
Inferior parietal lobule	L	40	−32	−52	42	2.89	2.55	0.005	
Fusiform gyrus	R	19	28	−68	−10	2.61	2.35	0.009	
Parahippocampal gyrus	L	28	−14	−44	2	2.52	2.28	0.011	
Lingual gyrus	R	37	28	−48	−6	2.42	2.20	0.014	
Cerebellum crus IV	R		2	−50	−16	2.4	2.19	0.014	
Calcarine cortex	L	17/18	−6	−66	18	2.36	2.15	0.016	
Parahippocampal gyrus	R	27	12	−38	−4	2.35	2.15	0.016	
Cerebellum crus VI	L		−2	−74	−10	2.3	2.11	0.018	
Mid temporal gyrus	R	21	58	−32	−10	3.58	3.03	0.001	222
Precentral gyrus	L	6	−36	−2	56	3.29	2.84	0.002	127
Postcentral gyrus	L	2	−64	−18	32	3.19	2.76	0.003	352
Superior temporal gyrus	L	42	−52	−14	14	2.84	2.52	0.006	
Mid temporal gyrus	L	21	−52	−46	−2	2.92	2.58	0.005	483
Mid temporal gyrus	L	21	−62	−26	2	2.39	2.18	0.015	
Inferior frontal gyrus	L	47	−40	40	−8	2.54	2.29	0.011	173
Inferior parietal lobule	R	40	38	−58	48	2.3	2.11	0.018	121
Negative									
Posterior mid cingulate cortex	L	31	−4	−18	42	3.33	2.86	0.002	850
Anterior cingulate cortex	L	24	−4	6	38	2.6	2.34	0.010	
Supplementary motor area	L	6	−4	−22	58	2.21	2.04	0.021	
Anterior cingulate cortex	R	32	2	28	30	1.95	1.83	0.034	
Superior frontal gyrus (medial)	R	10	8	60	6	3.19	2.76	0.003	2221
Superior frontal gyrus (medial)	R	6	2	12	60	3.17	2.75	0.003	
Superior frontal gyrus (medial)	R	9	6	62	30	3.03	2.65	0.004	
Superior frontal gyrus	R	8	12	28	60	2.88	2.54	0.005	
Anterior cingulate cortex (pregenual)	L	24	−14	46	−4	2.57	2.32	0.010	
Superior frontal gyrus (medial)	R	8	2	48	44	2.51	2.27	0.012	
Superior temporal gyrus	L	42	−48	−28	18	3.15	2.74	0.003	279
Inferior parietal lobule	L	40	−58	−40	34	2.82	2.50	0.006	
Putamen	R		16	16	−6	3	2.63	0.004	294
Putamen	R		24	−2	4	2.08	1.93	0.027	
Red nucleus			0	−22	2	2.99	2.62	0.004	208
Inferior parietal gyrus	R	40	56	−32	32	2.78	2.48	0.007	203
Thalamus	R		8	−14	14	2.72	2.43	0.008	311
Caudate nucleus	L		−10	−4	16	2.68	2.40	0.008	
Inferior temporal gyrus	R	37	34	−74	6	2.55	2.30	0.011	136
Parahippocampal gyrus	L	36	−30	2	−30	2.47	2.24	0.013	124
Putamen	L		−20	6	−8	2.08	1.94	0.026	
Cerebellum crus VII	L		−22	−70	−40	2.39	2.18	0.015	178
Anterior cingulate cortex (subgenual)	R	32	10	30	−8	2.37	2.16	0.015	213

Height threshold: T = 1.74, $P < 0.05$.
Extent threshold: $k = 120$.
L = left; R = right; BA = Brodmann area.

posterior cingulate cortex, precuneus, medial prefrontal cortex, anterior cingulate cortex, gyrus rectus, posterior insular cortex, superior temporal gyrus, and inferior temporal, parietal, and occipital gyri (Table 7 and Fig. 4A). The ASD group had higher functional connectivity strength in the hippocampus, inferior temporal gyrus, temporal pole, lingual gyrus, calcarine cortex and amygdala, all on the left, as well as the cerebellum bilaterally (Table 7 and Fig. 4B). A significant interaction (Group × SCR)

Table 4 Two-sample *t*-test between neurotypical control subjects and ASD for SCR correlations with brain activation

Region	L/R	BA	*x*	*y*	*z*	*T*	*Z*	*P*	*k*
Controls > ASD									
Superior temporal gyrus	L	42	−48	−28	18	3.89	3.48	0.000	202
Supramarginal gyrus	L	40	−58	−42	26	2.21	2.12	0.017	
Superior frontal gyrus (medial)	R	10	4	60	10	3.86	3.45	0.000	12511
Supplementary motor area	R	6	4	14	58	3.79	3.40	0.000	
Thalamus	R		10	−10	12	3.63	3.28	0.001	
Red nucleus	L		−2	−22	0	3.60	3.25	0.001	
Anterior cingulate cortex	L	24	−4	−18	42	3.46	3.15	0.001	
Anterior cingulate gyrus (pregenual)	L	32	−14	46	−4	3.42	3.11	0.001	
Caudate nucleus	L		−10	−4	16	3.08	2.85	0.002	
Anterior cingulate gyrus (subgenual)	R	32	10	30	−8	3.03	2.81	0.002	
Superior frontal gyrus (medial)	R	9	4	46	42	3.02	2.80	0.003	
Putamen	R		22	8	2	2.91	2.71	0.003	
Anterior cingulate cortex		24	0	6	32	2.85	2.66	0.004	
Anterior cingulate gyrus (pregenual)	R	24	6	38	10	2.82	2.63	0.004	
Caudate nucleus	L		−4	8	6	2.80	2.62	0.004	
Mid frontal gyrus	R	10	28	60	20	2.79	2.61	0.005	
Putamen	R		28	−8	6	2.71	2.55	0.005	
Anterior cingulate cortex	R	24	4	26	30	2.64	2.48	0.007	
Anterior insular cortex	R		28	18	−10	2.56	2.42	0.008	
Posterior cingulate cortex	L	31	−8	−38	46	2.55	2.41	0.008	
Inferior frontal gyrus	R	45	52	24	8	2.53	2.39	0.008	
Putamen	L		−20	6	−8	2.47	2.34	0.010	
Supplementary motor area	R	6	14	0	68	2.46	2.33	0.010	
Posterior cingulate cortex	R	31	16	−32	42	2.32	2.21	0.013	
Superior frontal gyrus	R	8	26	32	50	2.30	2.19	0.014	
Supplementary motor area	L	6	−10	8	72	2.29	2.18	0.015	
Mid frontal gyrus	R	46	42	28	42	2.27	2.16	0.015	
Mid frontal gyrus	R	6	36	4	38	3.00	2.79	0.003	679
Precentral gyrus	R	6	44	−6	50	2.57	2.42	0.008	
Cerebellum crus VIII	L		−20	−68	−38	2.98	2.77	0.003	410
Mid frontal gyrus	L	46	−24	46	26	2.90	2.70	0.003	351
Inferior occipital gyrus	R	19	42	−78	0	2.78	2.61	0.005	193
Supramarginal gyrus	R	40	56	−32	30	2.71	2.54	0.006	570
Anterior insular cortex	L		−38	24	4	2.45	2.33	0.010	172
Cerebellum crus IX	L		−4	−46	−46	2.34	2.23	0.013	202
Pons	L		−10	−20	−44	2.28	2.17	0.015	
ASD > Controls									
Cuneus	R	19	16	−82	20	3.96	3.52	0.000	5113
Lingual gyrus	R	18	14	−70	−2	3.56	3.23	0.001	
Superior parietal lobule	L	7	−30	−64	58	3.41	3.11	0.001	
Inferior parietal lobule	L	40	−46	−54	48	3.23	2.97	0.001	
Cerebellum crus VI	R		24	−56	−24	3.19	2.93	0.002	
Mid occipital gyrus	L	19	−44	−76	14	2.91	2.71	0.003	
Cerebellum crus IV	R		10	−50	−10	2.82	2.63	0.004	
Lingual gyrus	L	18	−8	−84	−6	2.80	2.62	0.004	
Calcarine sulcus	L	17	−4	−68	20	2.54	2.40	0.008	
Fusiform gyrus	L	19	−24	−62	−14	2.22	2.12	0.017	
Lingual gyrus	R	37	26	−44	−8	2.19	2.09	0.018	
Calcarine cortex	R	17	18	−64	14	2.12	2.03	0.021	
Cerebellum crus VI	L		−12	−72	−20	2.07	1.99	0.023	
Cerebellum crus IV	L		−8	−42	−4	2.03	1.96	0.025	
Postcentral gyrus	L	2	−64	−18	32	3.94	3.51	0.000	456
Precentral gyrus	L	6	−34	2	56	2.89	2.69	0.004	233
Mid temporal gyrus	L	21	−60	−34	4	2.88	2.69	0.004	487
Inferior frontal gyrus	L	45	−42	42	0	2.87	2.67	0.004	234
Mid temporal gyrus	R	21	64	−40	−4	2.80	2.62	0.004	233
Inferior parietal lobule	R	39	42	−64	44	2.35	2.24	0.013	139

Height threshold: T = 1.7, $P < 0.05$.
Extent threshold: $k = 120$.
L = left; R = right; BA = Brodmann area.

Table 5 Two sample *t*-test between neurotypical control subjects and ASD for the functional connectivity of the posterior cingulate cortex

Region	L/R	BA	*x*	*y*	*z*	*T*	*Z*	*P*	*k*
Controls > ASD									
Mid frontal gyrus	L	10	−24	44	22	5.35	4.45	0.000	7314
Superior frontal gyrus	R	10	16	52	20	4.34	3.79	0.000	
Anterior cingulate cortex	R	24	20	10	30	3.99	3.54	0.000	
Superior frontal gyrus	L	6	−14	16	60	3.29	3.01	0.001	
Anterior cingulate cortex (subgenual)	R	32	8	28	−4	3.27	3.00	0.001	
Superior frontal gyrus	L	6	−6	28	58	3.21	2.96	0.002	
Anterior cingulate cortex	R	32	14	28	30	3.18	2.92	0.002	
Mid frontal gyrus	L	6	−38	2	58	3.11	2.87	0.002	
Superior frontal gyrus	R	8	10	32	58	3.06	2.83	0.002	
Superior frontal gyrus (medial)		32	0	44	28	2.84	2.65	0.004	
Caudate nucleus	L		−6	2	12	2.58	2.43	0.007	
Caudate nucleus	R		6	2	14	2.49	2.36	0.009	
Orbitofrontal cortex	L	11	−6	38	−18	2.26	2.15	0.016	
Anterior cingulate cortex (subgenual)	L	32	−6	30	−4	2.17	2.07	0.019	
Caudate nucleus	L		−12	8	16	2.12	2.03	0.021	
Cerebral peduncle	R		14	−20	−32	3.56	3.23	0.001	
Cerebral peduncle	L		−18	−20	−30	3.34	3.06	0.001	
Posterior cingulate cortex	L	31	−10	−46	36	3.97	3.53	0.000	1852
Posterior cingulate cortex	R	31	8	−44	28	3.37	3.08	0.001	
Precuneus	R	7	2	−72	30	2.89	2.69	0.004	
Precuneus	L	7	−8	−62	36	2.49	2.36	0.009	
Temporal parietal junction	L	22	−52	−56	24	3.48	3.16	0.001	1193
Cerebellum crus II	R		32	−78	−46	3.42	3.12	0.001	682
Mid temporal gyrus	L	21	−64	−34	−10	3.37	3.08	0.001	783
Inferior temporal gyrus	L	21	−58	−22	−20	3.01	2.79	0.003	
Superior frontal gyrus	R	6	22	2	74	3.36	3.07	0.001	128
Mid temporal gyrus	L	21	−52	4	−34	3.02	2.80	0.003	147
Superior parietal lobule	R	7	14	−58	74	2.63	2.47	0.007	131
Inferior frontal gyrus	L	47	−50	34	−2	2.42	2.29	0.011	196
ASD > Controls									
Cuneus	L	18	−18	−92	14	4.55	3.94	0.000	16754
Superior occipital gyrus	L	19	−24	−80	14	4.47	3.88	0.000	
Inferior occipital gyrus	R	18	28	−86	−8	4.31	3.77	0.000	
Superior parietal lobule	R	7	26	−70	38	4.07	3.60	0.000	
Superior occipital gyrus	R	19	24	−70	24	3.94	3.51	0.000	
Fusiform gyrus	R	19	42	−70	−14	3.90	3.48	0.000	
Cerebellum crus IV	R		14	−40	−18	3.79	3.40	0.000	
Inferior longitudinal fasciculus	R	41	40	−30	0	3.71	3.34	0.000	
Medial occipital gyrus	R	18	28	−80	10	3.70	3.33	0.000	
Fusiform gyrus	R	19	32	−76	0	3.69	3.32	0.000	
Inferior temporal gyrus	R	37	52	−58	−10	3.64	3.29	0.001	
Cerebellum crus IV	R		2	−50	−2	3.22	2.96	0.002	
Superior occipital gyrus	R	19	16	−82	30	3.21	2.95	0.002	
Inferior occipital gyrus	R	19	40	−78	0	3.17	2.92	0.002	
Parahippocampal gyrus	R	36	28	0	−28	3.08	2.85	0.002	
Lingual gyrus	R	19	16	−76	−10	3.05	2.82	0.002	
Pons	R		10	−24	−26	2.91	2.71	0.003	
Hippocampus	L	34	−30	−20	−8	2.88	2.68	0.004	
Inferior occipital gyrus	L	19	−40	−80	2	2.87	2.67	0.004	
Pons	L		−2	−30	−14	2.86	2.67	0.004	
Fusiform gyrus	L	19	−28	−66	−14	2.78	2.60	0.005	
Superior parietal lobule	L	19	−22	−64	30	2.78	2.60	0.005	
Lingual gyrus	L	18	−8	−64	−4	2.77	2.59	0.005	
Amygdala	R		22	0	−18	2.66	2.50	0.006	
Temporal pole	R	38	32	8	−40	2.44	2.31	0.010	
Cerebellum crus VII	L	4/43	−8	−72	−36	3.53	3.21	0.001	450
Rolandic operculum	L		−40	−8	18	3.37	3.08	0.001	757

(continued)

Table 5 Continued

Region	L/R	BA	*x*	*y*	*z*	*T*	*Z*	*P*	*k*
Superior temporal gyrus	L	22	−64	−6	6	2.78	2.60	0.005	
Posterior insular cortex	L		−44	0	4	2.56	2.42	0.008	
Inferior frontal gyrus	R	45	48	20	8	3.15	2.90	0.002	945
Rolandic operculum	R	4/43	42	0	14	2.71	2.54	0.006	
Posterior insular cortex	R		44	8	2	2.35	2.24	0.013	
Temporal pole	L	38	−28	18	−34	3.14	2.90	0.002	227
Precentral gyrus	R	4	44	−10	34	2.91	2.71	0.003	412
Precentral gyrus	R	6	50	−4	46	2.72	2.55	0.005	
Postcentral gyrus	L	3	−42	−22	48	2.90	2.70	0.003	263
Supplementary motor area	L	6	−6	−4	60	2.88	2.68	0.004	424
Supplementary motor area	R	6	8	6	58	2.67	2.51	0.006	
Inferior parietal lobule	R	40	42	−38	60	2.69	2.53	0.006	309

Height threshold: T = 1.7, $P < 0.05$.
Extent threshold: $k = 120$.
L = left; R = right; BA = Brodmann area.

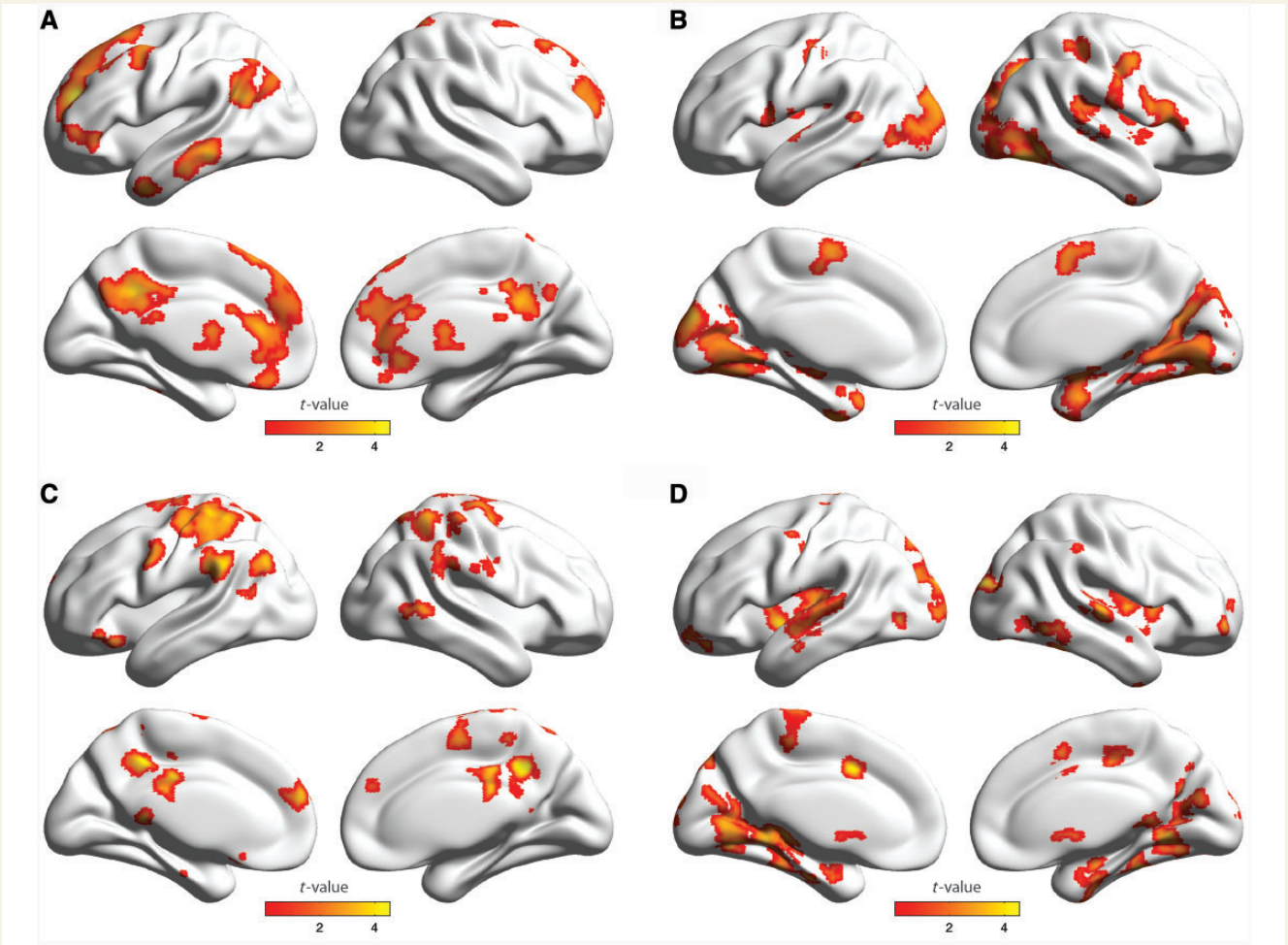

Figure 3 Functional connectivity of the posterior cingulate cortex, and an interaction between group (neurotypical controls versus ASD) and SCR (before versus after regressing out SCR signal) on posterior cingulate cortex connectivity. (**A**) Stronger connectivity in neurotypical controls compared with ASD (neurotypical controls > ASD). (**B**) Stronger connectivity in ASD, compared to neurotypical controls (ASD > neurotypical controls). (**C**) Stronger effects of SCR on posterior cingulate cortex connectivity in neurotypical control subjects compared to ASD [neurotypical controls (with-without SCR) > ASD (with-without SCR)]. (**D**) Stronger effects of SCR on posterior cingulate cortex connectivity in ASD compared with neurotypical control subjects [ASD (with-without SCR) > neurotypical controls (with-without SCR)].

Table 6 Interaction of group (neurotypical controls versus ASD) and SCR (with SCR versus without SCR) for the functional connectivity of the posterior cingulate cortex

Region	L/R	BA	*x*	*y*	*z*	*T*	*Z*	*P*	*k*
Controls (with-without) > ASD (with-without)									
Posterior cingulate cortex	R	31	6	−48	36	4.85	4.13	0.000	3566
Posterior cingulate cortex	L	31	−12	−40	40	4.63	3.99	0.000	
Superior parietal lobule	L	7	−34	−36	66	4.17	3.67	0.000	
Supramarginal gyrus	L	40	−62	−42	30	4.04	3.58	0.000	
Inferior parietal lobule	L	40	−42	−36	56	3.86	3.45	0.000	
Posterior cingulate cortex	R	23	4	−28	40	3.64	3.29	0.001	
Precuneus	R	7	2	−46	46	3.58	3.24	0.001	
Postcentral gyrus	L	3	−20	−38	54	3.22	2.96	0.002	
Postcentral gyrus	L	2	−42	−20	56	3.16	2.91	0.002	
Precentral gyrus	L	6	−36	−22	66	3.05	2.82	0.002	
Postcentral gyrus	R	2	62	−8	38	2.69	2.52	0.006	
Precentral gyrus	L	6	−54	0	44	4.07	3.60	0.000	266
Mid frontal gyrus	L	10	−8	54	20	3.98	3.54	0.000	443
Mid frontal gyrus		10	0	58	22	3.66	3.30	0.000	
Mid frontal gyrus	R	9	2	46	24	2.70	2.53	0.006	
Superior frontal gyrus	L	6	−14	−6	72	3.92	3.49	0.000	256
Gyrus rectus	L	11	−10	20	−16	3.11	2.87	0.002	
Cerebellum crus VIIIB	R		16	−58	−58	3.67	3.31	0.000	128
Posterior cingulate cortex	L	26	−6	−42	6	3.60	3.25	0.001	124
Cerebellum crus VI	R		14	−70	−24	3.57	3.23	0.001	264
Cerebellum crus I	R		36	−68	−30	2.91	2.71	0.003	
Angular gyrus	L	39	−46	−70	32	3.57	3.23	0.001	215
Dentate nucleus	R		12	−48	−26	3.48	3.16	0.001	178
Cerebellum crus I	L		−28	−88	−30	3.32	3.04	0.001	146
Superior parietal lobule	R	7	34	−48	58	3.28	3.01	0.001	895
Postcentral gyrus	R	2	16	−40	58	3.06	2.83	0.002	
Superior parietal lobule	R	7	20	−62	60	2.69	2.52	0.006	
Mid temporal gyrus	R	21	60	−52	4	3.05	2.82	0.002	
Inferior temporal gyrus	R	37	52	−62	2	2.58	2.43	0.008	
Precentral gyrus	R	6	26	−14	66	2.92	2.72	0.003	203
Mid frontal gyrus	R	6	30	−8	60	2.89	2.69	0.004	
Inferior frontal gyrus	L	47	−50	32	−14	2.88	2.69	0.004	126
Inferior frontal gyrus	L	47	−34	24	−16	2.80	2.62	0.004	
Supplementary motor area	R	6	8	−8	58	2.86	2.67	0.004	194
ASD (with-without) > Controls (with-without)									
Posterior insular cortex	R		42	−10	−12	4.98	4.21	0.000	1464
Putamen	R		26	−10	8	4.73	4.06	0.000	
Superior temporal gyrus	R	42	46	−28	6	3.30	3.02	0.001	
Posterior insular cortex	R		46	2	0	3.24	2.97	0.001	
Hippocampus	R	34	32	−10	−20	2.94	2.73	0.003	
Parahippocampal gyrus	R	28	30	−10	−32	2.62	2.47	0.007	
Amygdala	R		32	−2	−28	2.45	2.32	0.010	
Posterior insular cortex	L		−44	0	2	4.72	4.05	0.000	5420
Transverse temporal gyrus	L	41	−40	−26	6	4.66	4.00	0.000	
Fusiform gyrus	R	37	22	−52	−10	4.39	3.82	0.000	
Parahippocampal gyrus	L	28	−28	−22	−30	4.12	3.64	0.000	
Mid temporal gyrus	L	21	−50	−14	−4	3.84	3.44	0.000	
Lingual gyrus	R	19	14	−56	−4	3.81	3.41	0.000	
Lingual gyrus	L	19	−12	−70	0	3.80	3.40	0.000	
Hippocampus	L	34	−16	−32	−2	3.56	3.23	0.001	
Fusiform gyrus	L	20	−36	−32	−10	3.36	3.07	0.001	
Superior temporal gyrus	L	42	−56	−28	6	3.23	2.97	0.001	
Precuneus	R	31	6	−66	26	2.99	2.78	0.003	
Superior parietal lobule	L	19	−22	−80	46	2.94	2.74	0.003	
Calcarine cortex	L	17/18	−24	−64	4	2.91	2.71	0.003	
Precuneus	L	7	−2	−78	42	2.55	2.41	0.008	

(continued)

Table 6 Continued

Region	L/R	BA	x	y	z	T	Z	P	k
Anterior cingulate cortex	L	24	−12	8	38	4.36	3.80	0.000	512
Anterior cingulate cortex	R	24	2	6	42	3.10	2.86	0.002	
Superior occipital gyrus	R	19	22	−92	24	4.22	3.71	0.000	846
Superior occipital gyrus	L	18	−16	−96	20	3.96	3.52	0.000	
Mid occipital gyrus	R	18	30	−86	18	3.68	3.32	0.000	
Mid frontal gyrus	L	11	−34	62	−12	4.08	3.61	0.000	295
Fusiform gyrus	R	37	34	−38	−20	3.90	3.48	0.000	826
Inferior temporal gyrus	R	37	54	−62	−10	3.57	3.23	0.001	
Cerebellum crus I	R		50	−68	−28	3.33	3.05	0.001	
Superior temporal gyrus	R	22	66	−22	4	3.72	3.34	0.000	344
Mid frontal gyrus	R	10	36	52	−6	3.19	2.94	0.002	180
Paracentral lobule	L	4	−8	−28	68	2.59	2.44	0.007	170
Caudate nucleus	R		14	20	0	2.50	2.36	0.009	197

Height threshold: T = 1.7, $P < 0.05$.
Extent threshold: $k = 120$.
L = left; R = right; BA = Brodmann area.

was also found; SCR signal contributed significantly to the connectivity of the posterior cingulate cortex, medial prefrontal cortex, anterior cingulate cortex, inferior parietal lobule, and the right anterior and posterior insular cortex in neurotypical control subjects, compared with ASD (Table 8 and Fig. 4C). In ASD there was significant contribution of SCR signal to the connectivity of the hippocampus, amygdala, nucleus accumbens, calcarine cortex, and the fusiform, lingual, and inferior occipital gyri, compared with neurotypical control subjects (Table 8 and Fig. 4D). For within-group paired *t*-test results (before > after SCR regression), see Supplementary Table 4 and Supplementary Fig. 4.

Correlations with clinical symptoms

No significant correlations were found between the number of SCRs, or overall skin conductance level, and any of the four ADI-R subscales, all *P*'s > 0.05. However, ADI-R subscales for social interaction and communication were negatively correlated with posterior cingulate cortex connectivity with the medial and lateral prefrontal cortices, and with the posterior cingulate cortex and precuneus, respectively. Positive correlations with posterior cingulate cortex connectivity were found in sensory and temporal regions, as well as within the thalamus (Supplementary Table 5 and Supplementary Fig. 5) with all four subscales. Symptom severity on the social interaction and communication subscales was also correlated with decreased ventromedial prefrontal cortex connectivity with the posterior cingulate cortex (i.e. decreased DMN connectivity), as well as increased connectivity with the anterior insular cortex and anterior cingulate cortex (i.e. reduced anticorrelations with the task-positive network) (Supplementary Table 6 and Supplementary Fig. 6A and B). ADI-R correlations with whole brain connectivity revealed negative correlations with the posterior cingulate cortex/precuneus and supplementary motor area (social interaction and communication subscales), and positive correlations with the anterior cingulate cortex and medial prefrontal cortex (restricted behaviour and early development subscales) (Supplementary Table 7 and Supplementary Fig. 7). For ADI-R subscale correlation with brain activity that is associated with SCR, see Supplementary Table 8 and Supplementary Fig. 8.

Central generation and representation of skin conductance responses

One-sample *t*-tests of both generation and representation models revealed comparable brain activation associated with SCR to the original data in both groups (i.e. anterior brain regions in neurotypical controls, and posterior brain activation in ASD). When the two models were compared within each group, no significant differences were found between representation and generation (representation > generation) in neurotypical control subjects, or between the two models in ASD. There was, however, significant activation in the right thalamus and the left cerebellum in the generation model, as compared with the representation model (generation > representation), in neurotypical control subjects (Supplementary Table 9 and Supplementary Fig. 9).

Discussion

Skin conductance response and its correlations with brain activity

The results demonstrate a reduced number of spontaneous SCRs, as well as abnormal correlations of SCR with brain activation during rest in ASD. This could result from either abnormal peripheral conductance of autonomic nervous system signals, or from alterations in the central generation and/or representation of visceral autonomic arousal states. Previous studies have found abnormal basal autonomic nervous system activity in ASD (Horvath *et al.*, 1999; Molloy and Manning-Courtney, 2003; White, 2003; Ming *et al.*, 2005; Anderson and Colombo, 2009; Bal *et al.*, 2010; Anderson *et al.*, 2013). However, all of these findings indicate increased sympathetic/parasympathetic balance. Our finding of decreased number of SCRs in ASD, therefore, is unlikely to

Table 7 Two sample *t*-test between neurotypical controls and ASD for whole-brain functional connectivity

Region	L/R	BA	*x*	*y*	*z*	*T*	*Z*	*P*	*k*
Controls > ASD									
Superior temporal gyrus	R	38	42	6	−15	4.88	4.15	0.000	104
Posterior insular cortex	R		45	−12	0	3.03	2.81	0.002	
Inferior temporal gyrus	R	37	42	−63	−9	3.77	3.38	0.000	119
Inferior occipital gyrus	R	19	48	−75	0	3.31	3.03	0.001	
Gyrus rectus	L	11	−3	36	−18	3.75	3.37	0.000	361
Superior frontal gyrus (medial)	R	8	9	33	39	3.60	3.26	0.001	
Anterior cingulate cortex	L	32	−9	42	9	3.52	3.19	0.001	
Anterior cingulate cortex (subgenual)	R	32	6	30	−6	3.42	3.12	0.001	
Superior frontal gyrus (medial)	R	9	6	51	36	3.17	2.92	0.002	
Anterior cingulate cortex	R	24	12	36	9	3.08	2.85	0.002	
Superior frontal gyrus (medial)	L	9	−3	45	24	3.07	2.84	0.002	
Inferior parietal lobule	R	39	45	−54	36	3.45	3.14	0.001	101
Posterior cingulate cortex	L	23	−3	−36	39	3.34	3.05	0.001	376
Precuneus	L	31	−9	−57	36	2.74	2.57	0.005	
Precuneus	R	19	9	−54	30	2.56	2.42	0.008	
ASD > Controls									
Hippocampus	L		−30	−21	−12	4.61	3.98	0.000	120
Inferior temporal gyrus	L	20	−45	−27	−21	2.65	2.49	0.006	
Amygdala	L		−27	3	−18	2.29	2.18	0.015	
Calcarine cortex	L	17	−3	−63	9	4.02	3.57	0.000	79
Lingual gyrus	L	19	−12	−48	3	3.63	3.28	0.001	
Cerebellum crus VIII	L		−36	−63	−54	4.02	3.57	0.000	119
Cerebellum crus II	R		30	−78	−48	3.99	3.55	0.000	112
Temporal pole	L	38	−39	15	−30	2.99	2.77	0.003	
Cerebellum crus VII	L		−30	−39	−39	3.60	3.25	0.001	130
Cerebellum crus I	R		39	−57	−33	3.41	3.11	0.001	81

Height threshold: T = 1.7, $P < 0.05$.
Extent threshold: $k = 67$.
L = left, R = right; BA = Brodmann area.

be a result of hypoactivation of the sympathetic autonomic nervous system. Moreover, skin conductance level did not differ between groups, consistent with previous studies (Zahn *et al.*, 1987; Schoen *et al.*, 2008; Mathersul *et al.*, 2013), further suggesting that the electrodermal abnormality in ASD is not of peripheral origin. Thus, the results are likely to reflect alterations in the central generation and/or representation of SCR signals.

SCR is a sensitive index of sympathetic neural activity and can detect even subtle changes in autonomic arousal due to mental activity and thought processes (Nikula, 1991). Our results may, therefore, reflect differences in the central generation of SCR, stemming from different mental activity. More specifically, in neurotypical controls, SCR was positively correlated with the anterior insular cortex, a brain region involved in interoceptive awareness (Craig, 2002, 2009; Critchley *et al.*, 2002; Pollatos *et al.*, 2007; Gu *et al.*, 2013), and with the medial prefrontal cortex, which is implicated in self-referential processing (Craik *et al.*, 1999; Kelley *et al.*, 2002; Macrae *et al.*, 2004; Northoff *et al.*, 2006; Jenkins and Mitchell, 2011). In ASD, however, SCR was highly correlated with visual and auditory cortices. Thus, it is possible that when neurotypical control participants lay in the scanner at rest, they were aware of their inner bodily sensations and were engaged in self-referential thoughts, which drove their SCRs. On the other hand, when participants with ASD were resting in the scanner, they may have concentrated on the noises and the visual information inside the scanner and that may have been the driving force of their autonomic responses.

The results may also reflect alterations in the central representation of autonomic signals. The thalamus, supplementary motor area, anterior insular cortex, and anterior cingulate cortex were positively correlated with SCR in neurotypical controls, but were either not correlated, or negatively correlated with SCR in individuals with ASD. These brain regions were previously implicated in autonomic nervous system signal processing (Boucsein, 1992; Damasio *et al.*, 2000; Craig, 2002; Porges, 2003; Critchley, 2005; Gu *et al.*, 2013). The anterior insular cortex, specifically, was indicated to have a key role in the representation of autonomic signals. Anterior insular cortex was not associated with SCR in the ASD group, further supporting abnormal central autonomic nervous system representation in ASD.

Results from our additional analyses did not reveal significant differences in cortical regions that were uniquely associated with the generation or representation of SCR in both groups, suggesting the involvement of similar brain regions in both the generation and the representation of SCR. These regions corresponded with brain areas that were positively correlated with SCR in each of the groups in our original regression analysis, suggesting that the differences that were originally found between the groups are

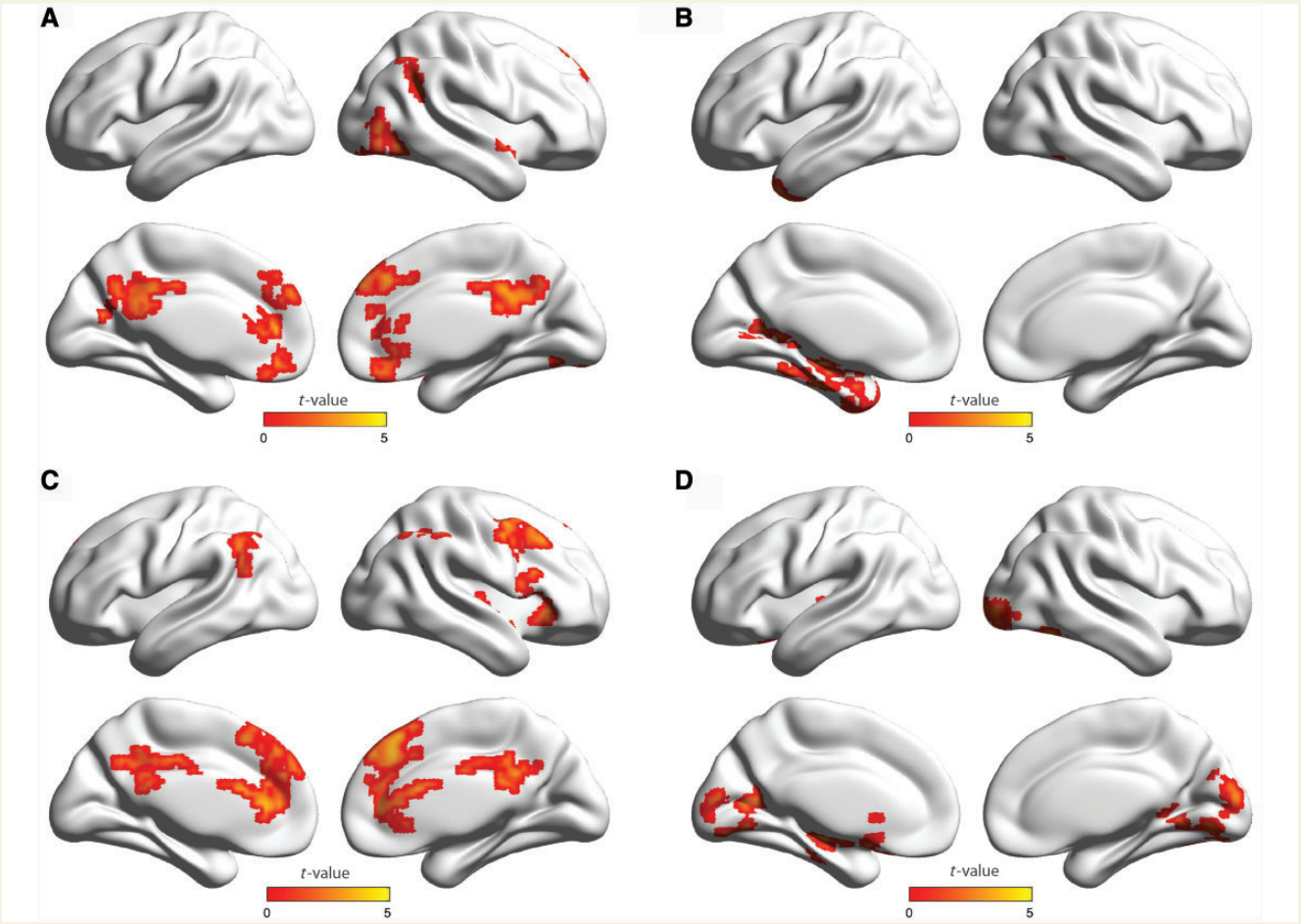

Figure 4 Voxel-wise whole brain functional connectivity, and an interaction between group (neurotypical controls versus ASD) and SCR (before versus after regressing out the SCR signal) in voxel-wise whole-brain connectivity. (**A**) Stronger connectivity in neurotypical controls compared with ASD (neurotypical controls > ASD). (**B**) Stronger connectivity in ASD, compared to neurotypical control subjects (ASD > neurotypical controls). (**C**) Stronger effects of SCR on whole-brain connectivity in neurotypical control subjects compared to ASD [neurotypical controls (with-without SCR) > ASD (with-without SCR)]. (**D**) Stronger effects of SCR on whole-brain connectivity in ASD compared to neurotypical control subjects [ASD (with-without SCR) > neurotypical controls (with-without SCR)].

present both in the generation phase and the representation phase of SCR signals. The higher activation in the right thalamus and left cerebellum that was found during the generation of SCRs in neurotypical controls may suggest that there is an increased autonomic arousal during the generation phase, compared with the representation phase. These results differ from previous findings of brain regions that are uniquely activated in the generation or representation of SCR in a healthy cohort (Critchley *et al.*, 2000). However, differences in methods may account for the discrepancy between the results of these studies. For a more detailed discussion of the afferent and efferent SCR pathways see the online Supplementary material.

Skin conductance response contribution to default mode network and voxel-wise connectivity

Our functional connectivity findings replicated recent work showing reduced connectivity of the DMN in individuals with ASD compared with neurotypical controls (Kennedy and Courchesne, 2008a, b; Monk *et al.*, 2009; Assaf *et al.*, 2010; Weng *et al.*, 2010), and added a critical component: the difference in DMN connectivity between the groups was significantly associated with SCR. Thus, by examining the interaction between SCR signal and group difference in posterior cingulate cortex connectivity, our data indicated significantly higher contributions of the SCR signal to the DMN connectivity in the neurotypical control group, compared to the ASD group. Decreased DMN connectivity in ASD was also found using the ventromedial prefrontal cortex as a seed; however, SCR did not have significant contributions to this network in this analysis. Because the ventromedial prefrontal cortex is a relatively large brain region, these negative results may be associated with the specific seed region of the ventromedial prefrontal cortex that was used in this analysis [based on the coordinates reported by Fox *et al.* (2005)]. Nevertheless, differences in autonomic-related brain activity may account, at least in part, for the previously observed under-connectivity of the DMN in ASD.

Table 8 Interaction of group (neurotypical controls versus ASD) and SCR (with SCR versus without SCR) for the functional connectivity of the whole brain

Region	L/R	BA	x	y	z	T	Z	P	k
Controls (with-without) > ASD (with-without)									
Anterior cingulate cortex	R	32	6	42	18	5.08	4.28	0.000	606
Superior frontal gyrus (medial)	L	8	−3	30	60	4.13	3.65	0.000	
Superior frontal gyrus (medial)	R	8	6	33	42	4.03	3.57	0.000	
Anterior cingulate cortex (pregenual)	L	24	−6	33	6	3.95	3.51	0.000	
Anterior cingulate cortex (subgenual)	R	25	6	24	−6	2.96	2.75	0.003	
Inferior frontal gyrus	R	45	48	21	3	4.17	3.67	0.000	157
Anterior insular cortex	R		33	21	−9	2.76	2.59	0.005	
Posterior insular cortex	R		42	−15	−6	4.13	3.65	0.000	78
Cerebellum crus II	L		−9	−84	−24	3.26	2.99	0.001	87
Mid frontal gyrus	R	8	33	15	54	3.20	2.95	0.002	197
Mid frontal gyrus	R	8	42	24	42	3.08	2.85	0.002	
Posterior cingulate cortex		23	0	−12	30	3.20	2.94	0.002	230
Posterior cingulate cortex	R	26	3	−42	27	2.97	2.76	0.003	
Posterior cingulate cortex	L	31	−3	−27	36	2.89	2.69	0.004	
Precuneus	L	31	−12	−57	36	2.81	2.62	0.004	
Inferior parietal lobule	L	40	−51	−51	39	3.12	2.88	0.002	99
Angular gyrus	L	39	−57	−60	27	2.58	2.43	0.007	
Inferior parietal lobule	R	40	36	−51	42	2.96	2.75	0.003	92
Vermis IV	R		6	−54	−21	2.64	2.48	0.007	78
ASD (with-without) > Controls (with-without)									
Hippocampus	L		−30	−21	−12	4.43	3.86	0.000	74
Amygdala	L		−21	−3	−15	2.16	2.07	0.019	
Cerebellum crus VII	R		39	−69	−54	2.76	2.58	0.005	80
Nucleus accumbens	L		−21	9	−15	3.67	3.31	0.000	92
Caudate nucleus	L		−6	12	−3	3.08	2.85	0.002	
Calcarine cortex	R	18	3	−90	12	3.53	3.20	0.001	203
Calcarine cortex	L	17	−9	−66	9	3.34	3.05	0.001	
Cuneus	L	19	3	−81	36	2.51	2.37	0.009	
Cerebellum crus VI	L		−12	−72	−18	3.19	2.93	0.002	92
Inferior occipital gyrus	L	18	−18	−90	−6	2.33	2.22	0.013	
Fusiform gyrus	R	37	42	−60	−15	3.11	2.87	0.002	145
Lingual gyrus	R	18	15	−54	0	2.93	2.73	0.003	
Inferior occipital gyrus	R	18	33	−93	−12	3.06	2.83	0.002	109

Height threshold: T = 1.7, $P < 0.05$.
Extent threshold: $k = 67$.
L = left; R = right; BA = Brodmann area.

Voxel-wise whole-brain connectivity analysis results were strikingly similar to those obtained for the posterior cingulate cortex connectivity analysis, providing converging evidence for a decreased connectivity in DMN-related brain regions, and increased connectivity along the medial temporal lobe in ASD. Moreover, symptom severity on the social interaction and communication subscales of the ADI-R were negatively correlated with DMN connectivity strength in the posterior cingulate cortex, ventromedial prefrontal cortex and whole brain connectivity analyses. The analysis of the interaction between whole-brain connectivity and SCR revealed significant contributions of SCR signals to the connectivity patterns in both groups, suggesting that differences in autonomic-related brain activity between the groups may account, at least in part, for the differences in brain connectivity.

Possible differences in thought content, as previously discussed, may also account for the differences in DMN connectivity. Previous studies have linked the DMN to the generation of spontaneous thoughts (Mason *et al.*, 2007; Andrews-Hanna *et al.*, 2010) and self-referential mental activity (Whitfield-Gabrieli *et al.*, 2011). Thus, the weaker connectivity of the DMN and higher connectivity of visual and auditory cortices in ASD may indicate an inability to shift attention from exteroceptive to interoceptive signals during rest in those individuals. This interpretation supports a recent model in which ASD is associated with abnormalities in the salience network (Uddin and Menon, 2009; Menon and Uddin, 2010). The salience network is comprised of the anterior insular cortex and anterior cingulate cortex, and is postulated to play a key role in switching between the externally oriented executive control network and the internally oriented DMN (Uddin and Menon, 2009; Menon and Uddin, 2010). Indeed, several studies have found neuropathological and functional abnormalities of the anterior insular cortex in ASD (Di Martino *et al.*, 2009; Ebisch *et al.*, 2011; Santos *et al.*, 2011), and altered

functional connectivity patterns of the anterior insular cortex in the ASD group were found in our data set too. It is possible, therefore, that the focus of the ASD participants on visual and auditory information during the scan may have not only driven their SCR, but in fact influenced whole brain connectivity patterns, including connectivity of the DMN. This model, together with the significant contributions of SCR to the connectivity patterns, supports the importance of autonomic activity in modulating resting-state functional connectivity.

This work adds an important element to an emerging line of research showing significant contributions of autonomic nervous system signals to resting state network connectivity in the normal population (Birn *et al.*, 2008; Iacovella and Hasson, 2011; Fan *et al.*, 2012). These studies suggest that incorporating measurements of autonomic signals in resting-state functional MRI connectivity analysis, rather than regressing them out as noise, may provide better insight into the driving forces of brain fluctuations, and the representation of brain activity and connectivity during 'rest'. The current findings further suggest that examining autonomic nervous system contributions to brain connectivity during rest may significantly improve our understanding of alterations in resting state functional connectivity patterns that were previously observed in a variety of patient populations, such as in individuals with depression (Greicius *et al.*, 2007; Bluhm *et al.*, 2009), schizophrenia (Garrity *et al.*, 2007; Whitfield-Gabrieli *et al.*, 2009; Öngür *et al.*, 2010), bipolar disorder (Ongur *et al.*, 2010) and attention-deficit hyperactivity disorder (Uddin *et al.*, 2008; Cao *et al.*, 2009), in addition to ASD (Kennedy and Courchesne, 2008b; Monk *et al.*, 2009; Assaf *et al.*, 2010; Weng *et al.*, 2010).

Clinical implications

Our data may have important clinical implications for the diagnosis and treatment of ASD. Autonomic measures are relatively easy and inexpensive to obtain, even with individuals of a very young age. Detecting autonomic abnormalities may aid in an early diagnosis of ASD, a process that could be critical to the effectiveness of existing behavioural treatments (Eaves and Ho, 2004; Granpeesheh *et al.*, 2009). In addition, treatments targeting autonomic abnormalities may also reduce autistic symptoms (Murphy *et al.*, 2000; Binstock, 2001; Porges, 2003; Field and Diego, 2008). For example, Murphy *et al.* (2000) observed that autistic symptoms were significantly reduced after vagal nerve stimulation in four patients with severe autistic behaviours. More research is needed, however, to determine the benefits of such treatments for ASD.

Conclusion

Our data provide evidence for abnormal associations between spontaneous SCR and brain activity and connectivity during rest in ASD. The observed autonomic abnormalities may contribute to the socio-emotional deficits in ASD because autonomic signals are essential to emotional processing. Taking autonomic measurements during investigation of resting state brain activity and connectivity may be critical for between-group comparisons, especially if one of the groups exhibits emotional abnormality, as is the case in many forms of psychopathology.

Funding

This research was supported by the National Institute of Health (NIH) Grant R21 MH083164 and two Research Enhancement Awards from Queens College, City University of New York, to J.F., along with the National Center for Research Resources (NCRR) Grant UL1 RR029887, and a James S. McDonnell Foundation grant (22002078, to P.R.H.). Two additional grants, from the National Natural Science Foundation (Grant No. 81030028) and the National Science Fund for Distinguished Young Scholars (Grant No. 81225012) of China to Y.H., helped in supporting this study. The contents are the sole responsibility of the authors and do not necessarily represent the official views of the aforementioned funding agencies. We would like to acknowledge the Beatrice and Samuel A. Seaver Foundation for their support. The authors report no biomedical financial interests or potential conflicts of interest.

Supplementary material

Supplementary material is available at *Brain* online.

References

Adolphs R. Neural systems for recognizing emotion. Curr Opin Neurobiol 2002; 12: 169–77.

American Psychiatric Association. DSM-5 Task Force. Diagnostic and statistical manual of mental disorders. DSM-5. 5th edn. Arlington, VA: American Psychiatric Association; 2013.

Anderson CJ, Colombo J. Larger tonic pupil size in young children with autism spectrum disorder. Dev Psychobiol 2009; 51: 207–11.

Anderson CJ, Colombo J, Unruh KE. Pupil and salivary indicators of autonomic dysfunction in autism spectrum disorder. Dev Psychobiol 2013; 55: 465–82.

Andrews-Hanna JR, Reidler JS, Huang C, Buckner RL. Evidence for the default network's role in spontaneous cognition. J Neurophysiol 2010; 104: 322–35.

Assaf M, Jagannathan K, Calhoun VD, Miller L, Stevens MC, Sahl R, et al. Abnormal functional connectivity of default mode sub-networks in autism spectrum disorder patients. NeuroImage 2010; 53: 247–56.

Bach DR, Daunizeau J, Friston KJ, Dolan RJ. Dynamic causal modelling of anticipatory skin conductance responses. Biol Psychol 2010a; 85: 163–70.

Bach DR, Flandin G, Friston KJ, Dolan RJ. Modelling event-related skin conductance responses. Int J Psychophysiol 2010b; 75: 349–56.

Bal E, Harden E, Lamb D, Van Hecke AV, Denver JW, Porges SW. Emotion recognition in children with autism spectrum disorders: relations to eye gaze and autonomic state. J Autism Dev Disord 2010; 40: 358–70.

Baron-Cohen S. Do people with autism understand what causes emotion? Child Dev 1991; 62: 385–95.

Barrett LF, Mesquita B, Ochsner KN, Gross JJ. The experience of emotion. Annu Rev Psychol 2007; 58: 373–403.

Binstock T. Anterior insular cortex: linking intestinal pathology and brain function in autism-spectrum subgroups. Med Hypotheses 2001; 57: 714–17.

Birn RM, Murphy K, Bandettini PA. The effect of respiration variations on independent component analysis results of resting state functional connectivity. Hum Brain Mapp 2008; 29: 740–50.
Bluhm R, Williamson P, Lanius R, Theberge J, Densmore M, Bartha R, et al. Resting state default-mode network connectivity in early depression using a seed region-of-interest analysis: decreased connectivity with caudate nucleus. Psychiatry Clin Neurosci 2009; 63: 754–61.
Boucsein W. Electrodermal activity. New York: Plenum; 1992.
Buckner RL, Sepulcre J, Talukdar T, Krienen FM, Liu H, Hedden T, et al. Cortical hubs revealed by intrinsic functional connectivity: mapping, assessment of stability, and relation to Alzheimer's disease. J Neurosci 2009; 29: 1860–73.
Cao X, Cao Q, Long X, Sun L, Sui M, Zhu C, et al. Abnormal resting-state functional connectivity patterns of the putamen in medication-naive children with attention deficit hyperactivity disorder. Brain Res 2009; 1303: 195–206.
Chang C, Metzger CD, Glover GH, Duyn JH, Heinze HJ, Walter M. Association between heart rate variability and fluctuations in resting-state functional connectivity. NeuroImage 2013; 68: 93–104.
Cole MW, Pathak S, Schneider W. Identifying the brain's most globally connected regions. NeuroImage 2010; 49: 3132–48.
Craig AD. How do you feel? Interoception: the sense of the physiological condition of the body. Nat Rev Neurosci 2002; 3: 655–66.
Craig AD. Interoception: the sense of the physiological condition of the body. Curr Opin Neurobiol 2003; 13: 500–5.
Craig AD. How do you feel–now? The anterior insula and human awareness. Nat Rev Neurosci 2009; 10: 59–70.
Craik FIM, Moroz TM, Moscovitch M, Stuss DT, Winocur G, Tulving E, et al. In search of the self: a positron emission tomography study. Psychol Sci 1999; 10: 26–34.
Critchley HD. Neural mechanisms of autonomic, affective, and cognitive integration. J Comp Neurol 2005; 493: 154–66.
Critchley HD, Elliott R, Mathias CJ, Dolan RJ. Neural activity relating to generation and representation of galvanic skin conductance responses: a functional magnetic resonance imaging study. J Neurosci 2000; 20: 3033–40.
Critchley HD, Melmed RN, Featherstone E, Mathias CJ, Dolan RJ. Volitional control of autonomic arousal: a functional magnetic resonance study. NeuroImage 2002; 16: 909–19.
Critchley HD, Nagai Y, Gray MA, Mathias CJ. Dissecting axes of autonomic control in humans: insights from neuroimaging. Auton Neurosci 2011; 161: 34–42.
Damasio AR, Grabowski TJ, Bechara A, Damasio H, Ponto LL, Parvizi J, et al. Subcortical and cortical brain activity during the feeling of self-generated emotions. Nat Neurosci 2000; 3: 1049–56.
Di Martino A, Ross K, Uddin LQ, Sklar AB, Castellanos FX, Milham MP. Functional brain correlates of social and nonsocial processes in autism spectrum disorders: an activation likelihood estimation meta-analysis. Biol Psychiatry 2009; 65: 63–74.
Eaves LC, Ho HH. The very early identification of autism: outcome to age 4 1/2-5. J Autism Dev Disord 2004; 34: 367–78.
Ebisch SJ, Gallese V, Willems RM, Mantini D, Groen WB, Romani GL, et al. Altered intrinsic functional connectivity of anterior and posterior insula regions in high-functioning participants with autism spectrum disorder. Hum Brain Mapp 2011; 32: 1013–28.
Ekman P, Levenson RW, Friesen WV. Autonomic nervous-system activity distinguishes among emotions. Science 1983; 221: 1208–10.
Fan J, Xu P, Van Dam NT, Eilam-Stock T, Gu X, Luo YJ, et al. Spontaneous brain activity relates to autonomic arousal. J Neurosci 2012; 32: 11176–86.
Field T, Diego M. Vagal activity, early growth and emotional development. Infant Behav Dev 2008; 31: 361–73.
Fox MD, Snyder AZ, Vincent JL, Corbetta M, Van Essen DC, Raichle ME. The human brain is intrinsically organized into dynamic, anticorrelated functional networks. Proc Natl Acad Sci USA 2005; 102: 9673–8.
Friston KJ, Holmes AP, Worsley KJ, Poline J-P, Frith CD, Frackowiak RSJ. Statistical parametric maps in functional imaging: a general linear approach. Hum Brain Mapp 1995; 2: 189–210.
Frith CD, Frith U. Social cognition in humans. Curr Biol 2007; 17: R724–32.
Garrity AG, Pearlson GD, McKiernan K, Lloyd D, Kiehl KA, Calhoun VD. Aberrant "default mode" functional connectivity in schizophrenia. Am J Psychiatry 2007; 164: 450–7.
Gray MA, Harrison NA, Wiens S, Critchley HD. Modulation of emotional appraisal by false physiological feedback during fMRI. PLoS one 2007; 2: e546.
Granpeesheh D, Dixon DR, Tarbox J, Kaplan AM, Wilke AE. The effects of age and treatment intensity on behavioral intervention outcomes for children with autism spectrum disorders. Res Autism Spectr Disord 2009; 3: 1014–22.
Greicius MD, Flores BH, Menon V, Glover GH, Solvason HB, Kenna H, et al. Resting-state functional connectivity in major depression: abnormally increased contributions from subgenual cingulate cortex and thalamus. Biol Psychiatry 2007; 62: 429–37.
Gu X, Gao Z, Wang X, Liu X, Knight RT, Hof PR, et al. Anterior insular cortex is necessary for empathetic pain perception. Brain 2012; 135 (Pt 9): 2726–35.
Gu X, Hof PR, Friston KJ, Fan J. Anterior insular cortex and emotional awareness. J Comp Neurol 2013; 521: 3371–88.
Harrison NA, Gray MA, Gianaros PJ, Critchley HD. The embodiment of emotional feelings in the brain. J Neurosci 2010; 30: 12878–84.
Hill E, Berthoz S, Frith U. Brief report: cognitive processing of own emotions in individuals with autistic spectrum disorder and in their relatives. J Autism Dev Disord 2004; 34: 229–35.
Hirstein W, Iversen P, Ramachandran VS. Autonomic responses of autistic children to people and objects. Proc Biol Sci 2001; 268: 1883–8.
Hobson RP, Ouston J, Lee A. Emotion recognition in autism: coordinating faces and voices. Psychol Med 1988; 18: 911–23.
Horvath K, Papadimitriou JC, Rabsztyn A, Drachenberg C, Tildon JT. Gastrointestinal abnormalities in children with autistic disorder. J Pediatr 1999; 135: 559–63.
Iacovella V, Hasson U. The relationship between BOLD signal and autonomic nervous system functions: implications for processing of "physiological noise". J Magn Reson Imag 2011; 29: 1338–45.
James W. What is an emotion? Mind 1884; 9: 188–205.
Jenkins AC, Mitchell JP. Medial prefrontal cortex subserves diverse forms of self-reflection. Soc Neurosci 2011; 6: 211–18.
Kelley WM, Macrae CN, Wyland CL, Caglar S, Inati S, Heatherton TF. Finding the self? An event-related fMRI study. J Cogn Neurosci 2002; 14: 785–94.
Kennedy DP, Courchesne E. Functional abnormalities of the default network during self- and other-reflection in autism. Soc Cogn Affect Neurosci 2008a; 3: 177–90.
Kennedy DP, Courchesne E. The intrinsic functional organization of the brain is altered in autism. NeuroImage 2008b; 39: 1877–85.
Koshino H, Carpenter PA, Minshew NJ, Cherkassky VL, Keller TA, Just MA. Functional connectivity in an fMRI working memory task in high-functioning autism. Neuroimage 2005; 24: 810–21.
Kylliainen A, Hietanen JK. Skin conductance responses to another person's gaze in children with autism. J Autism Dev Disord 2006; 36: 517–25.
Lange CG. The mechanism of the emotions. In: Rand B, editor. The classical psychologist. Boston, MA: Houghton Mifflin; 1885. p. 672–85.
Ledberg A, Akerman S, Roland PE. Estimation of the probabilities of 3D clusters in functional brain images. NeuroImage 1998; 8: 113–28.
Liang X, Zou Q, He Y, Yang Y. Coupling of functional connectivity and regional cerebral blood flow reveals a physiological basis for network hubs of the human brain. Proc Natl Acad Sci USA 2013; 110: 1929–34.
Liebhart EH. Effects of false heart rate feedback and task instructions on information search, attributions, and stimulus ratings. Psychol Res 1977; 39: 185–202.
Lord C, Risi S, Lambrecht L, Cook EH Jr, Leventhal BL, DiLavore PC, et al. The autism diagnostic observation schedule-generic: a standard

measure of social and communication deficits associated with the spectrum of autism. J Autism Dev Disord 2000; 30: 205–23.
Lord C, Rutter M, Le Couteur A. Autism diagnostic interview-revised: a revised version of a diagnostic interview for caregivers of individuals with possible pervasive developmental disorders. J Autism Dev Disord 1994; 24: 659–85.
Macrae CN, Moran JM, Heatherton TF, Banfield JF, Kelley WM. Medial prefrontal activity predicts memory for self. Cereb Cortex 2004; 14: 647–54.
Mason MF, Norton MI, Van Horn JD, Wegner DM, Grafton ST, Macrae CN. Wandering minds: the default network and stimulus-independent thought. Science 2007; 315: 393–5.
Mathersul D, McDonald S, Rushby JA. Autonomic arousal explains social cognitive abilities in high-functioning adults with autism spectrum disorder. Int J Psychophysiol 2013; 89: 475–482.
Menon V, Uddin LQ. Saliency, switching, attention and control: a network model of insula function. Brain Struct Funct 2010; 214: 655–67.
Ming X, Julu PO, Brimacombe M, Connor S, Daniels ML. Reduced cardiac parasympathetic activity in children with autism. Brain Dev 2005; 27: 509–16.
Molloy CA, Manning-Courtney P. Prevalence of chronic gastrointestinal symptoms in children with autism and autistic spectrum disorders. Autism 2003; 7: 165–71.
Monk CS, Peltier SJ, Wiggins JL, Weng SJ, Carrasco M, Risi S, et al. Abnormalities of intrinsic functional connectivity in autism spectrum disorders. NeuroImage 2009; 47: 764–72.
Murphy JV, Wheless JW, Schmoll CM. Left vagal nerve stimulation in six patients with hypothalamic hamartomas. Pediatr Neurol 2000; 23: 167–8.
Nikula R. Psychological correlates of nonspecific skin conductance responses. Psychophysiology 1991; 28: 86–90.
Northoff G, Heinzel A, de Greck M, Bermpohl F, Dobrowolny H, Panksepp J. Self-referential processing in our brain–a meta-analysis of imaging studies on the self. NeuroImage 2006; 31: 440–57.
Öngür D, Lundy M, Greenhouse I, Shinn AK, Menon V, Cohen BM, et al. Default mode network abnormalities in bipolar disorder and schizophrenia. Psychiatry Res 2010; 183: 59–68.
Patterson JC II, Ungerleider LG, Bandettini PA. Task-independent functional brain activity correlation with skin conductance changes: an fMRI study. NeuroImage 2002; 17: 1797–806.
Phillips ML, Drevets WC, Rauch SL, Lane R. Neurobiology of emotion perception I: the neural basis of normal emotion perception. Biol Psychiatry 2003; 54: 504–14.
Pollatos O, Gramann K, Schandry R. Neural systems connecting interoceptive awareness and feelings. Hum Brain Mapp 2007; 28: 9–18.
Porges SW. The polyvagal theory: phylogenetic contributions to social behavior. Physiol Behav 2003; 79: 503–13.
Rainville P, Bechara A, Naqvi N, Damasio AR. Basic emotions are associated with distinct patterns of cardiorespiratory activity. Int J Psychophysiol 2006; 61: 5–18.
Santos M, Uppal N, Butti C, Wicinski B, Schmeidler J, Giannakopoulos P, et al. Von Economo neurons in autism: a stereologic study of the frontoinsular cortex in children. Brain Res 2011; 1380: 206–17.
Schoen SA, Miller LJ, Brett-Green B, Hepburn SL. Psychophysiology of children with autism spectrum disorder. Res Autism Spectr Disord 2008; 2: 417–29.
Seth AK, Suzuki K, Critchley HD. An interoceptive predictive coding model of conscious presence. Front Psychol 2011; 2: 395.
Silani G, Bird G, Brindley R, Singer T, Frith C, Frith U. Levels of emotional awareness and autism: an fMRI study. Soc Neurosci 2008; 3: 97–112.
Slotnick SD, Schacter DL. A sensory signature that distinguishes true from false memories. Nat Neurosci 2004; 7: 664–72.
Song XW, Dong ZY, Long XY, Li SF, Zuo XN, Zhu CZ, et al. REST: a toolkit for resting-state functional magnetic resonance imaging data processing. PLoS ONE 2011; 6: e25031.
Truax SR. Active search, mediation, and the manipulation os cue dimensions: emotion attribution in the false feedback paradigm. Motiv Emot 1983; 7: 41–59.
Tzourio-Mazoyer N, Landeau B, Papathanassiou D, Crivello F, Etard O, Delcroix N, et al. Automated anatomical labeling of activations in SPM using a macroscopic anatomical parcellation of the MNI MRI single-subject brain. Neuroimage 2002; 15: 273–89.
Uddin LQ, Kelly AM, Biswal BB, Margulies DS, Shehzad Z, Shaw D, et al. Network homogeneity reveals decreased integrity of default-mode network in ADHD. J Neurosci Methods 2008; 169: 249–54.
Uddin LQ, Menon V. The anterior insula in autism: under-connected and under-examined. Neurosci Biobehav Rev 2009; 33: 1198–203.
Valins S. Cognitive effects of false heart-rate feedback. J Pers Soc Psychol 1966; 4: 400–8.
Van Dijk KR, Hedden T, Venkataraman A, Evans KC, Lazar SW, Buckner RL. Intrinsic functional connectivity as a tool for human connectomics: theory, properties, and optimization. J Neurophysiol 2010; 103: 297–321.
Vaughan Van Hecke A, Lebow J, Bal E, Lamb D, Harden E, Kramer A, et al. Electroencephalogram and heart rate regulation to familiar and unfamiliar people in children with autism spectrum disorders. Child Dev 2009; 80: 1118–33.
Vetrugno R, Liguori R, Cortelli P, Montagna P. Sympathetic skin response: basic mechanisms and clinical applications. Clin Auton Res 2003; 13: 256–70.
Vogt BA. Pain and emotion interactions in subregions of the cingulate gyrus. Nat Rev Neurosci 2005; 6: 533–44.
Wang L, Dai Z, Peng H, Tan L, Ding Y, He Z, et al. Overlapping and segregated resting-state functional connectivity in patients with major depressive disorder with and without childhood neglect. Hum Brain Mapp 2013; doi: 10.1002/hbm.22241.
Wechsler D. Wechsler adult intelligence scale. 3rd edn. New York: Psychological Corporation; 1997.
Weng SJ, Wiggins JL, Peltier SJ, Carrasco M, Risi S, Lord C, et al. Alterations of resting state functional connectivity in the default network in adolescents with autism spectrum disorders. Brain Res 2010; 1313: 202–14.
White JF. Intestinal pathophysiology in autism. Exp Biol Med (Maywood) 2003; 228: 639–49.
Whitfield-Gabrieli S, Moran JM, Nieto-Castanon A, Triantafyllou C, Saxe R, Gabrieli JD. Associations and dissociations between default and self-reference networks in the human brain. NeuroImage 2011; 55: 225–32.
Whitfield-Gabrieli S, Thermenos HW, Milanovic S, Tsuang MT, Faraone SV, McCarley RW, et al. Hyperactivity and hyperconnectivity of the default network in schizophrenia and in first-degree relatives of persons with schizophrenia. Proc Natl Acad Sci USA 2009; 106: 1279–84.
Xia M, Wang J, He Y. BrainNet Viewer: A Network Visualization Tool for Human Brain Connectomics. PLoS ONE 2013; 8 (7): e68910.
Yan C-G, Zang Y-F. DPARSF: a MATLAB toolbox for "pipeline" data analysis of resting-state fMRI. Front Syst Neurosci 2010; 4: 13.
Zahn TP, Rumsey JM, Van Kammen DP. Autonomic nervous system activity in autistic, schizophrenic, and normal men: effects of stimulus significance. J Abnorm Psychol 1987; 96: 135–44.
Zuo XN, Ehmke R, Mennes M, Imperati D, Castellanos FX, Sporns O, et al. Network centrality in the human functional connectome. Cereb Cortex 2012; 22: 1862–75.